

The measurement of the wavelength-dependent water transparency in Super-Kamiokande

Tomoaki Tada Okayama University, Japan (tadatomo2976@s.okayama-u.ac.jp)

Seunghyun Jung Seoul National University, South Korea

Minwoo Lee Sungkyunkwan University, South Korea

Ji-Woong Seo Sungkyunkwan University, South Korea

On behalf of Super-Kamiokande Collaboration

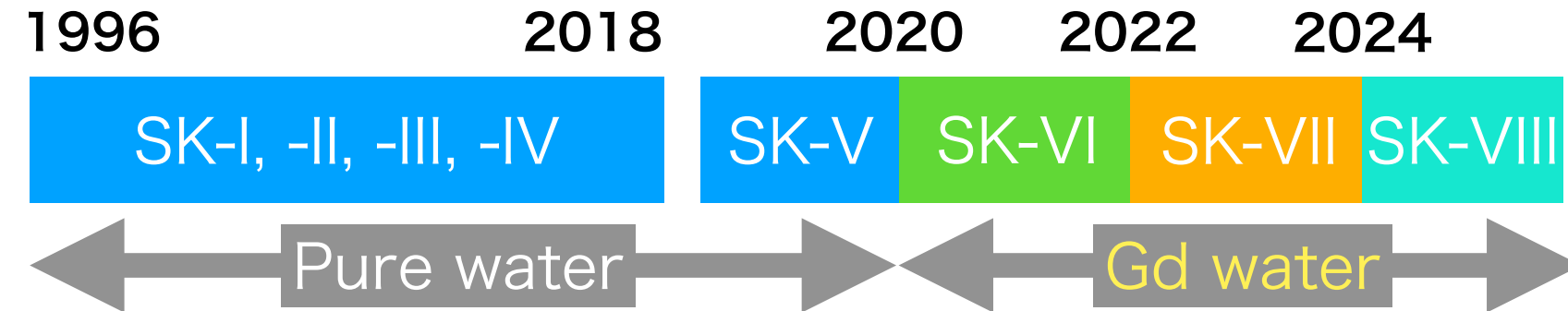
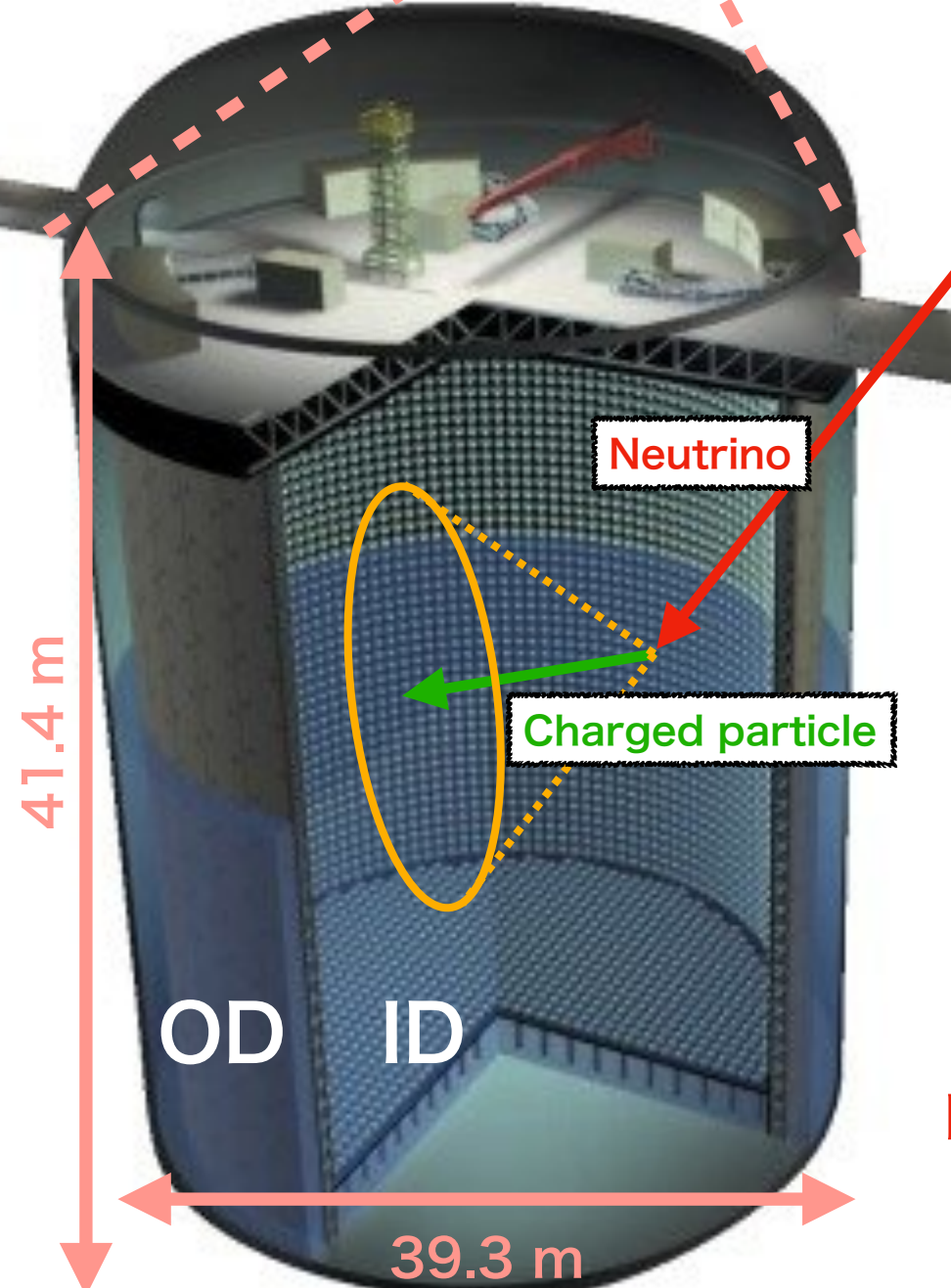
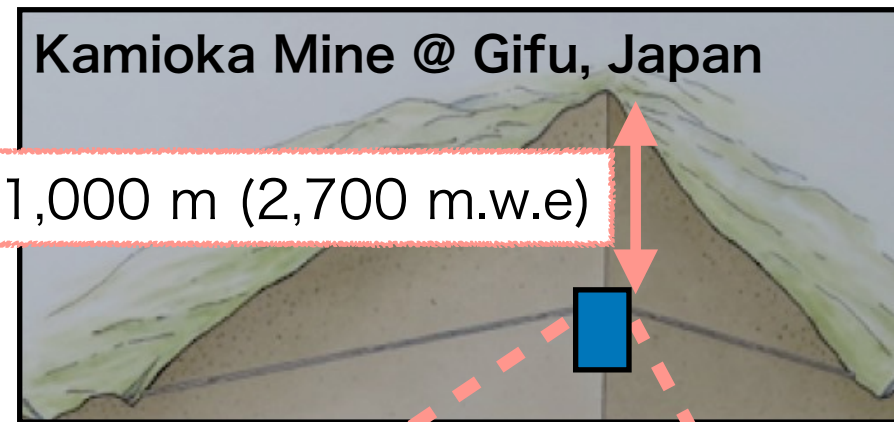
The 19th International Conference on Topic in Astroparticle and Underground Physics (TAUP2025)

@ Xichang, China

August 27th, 2025



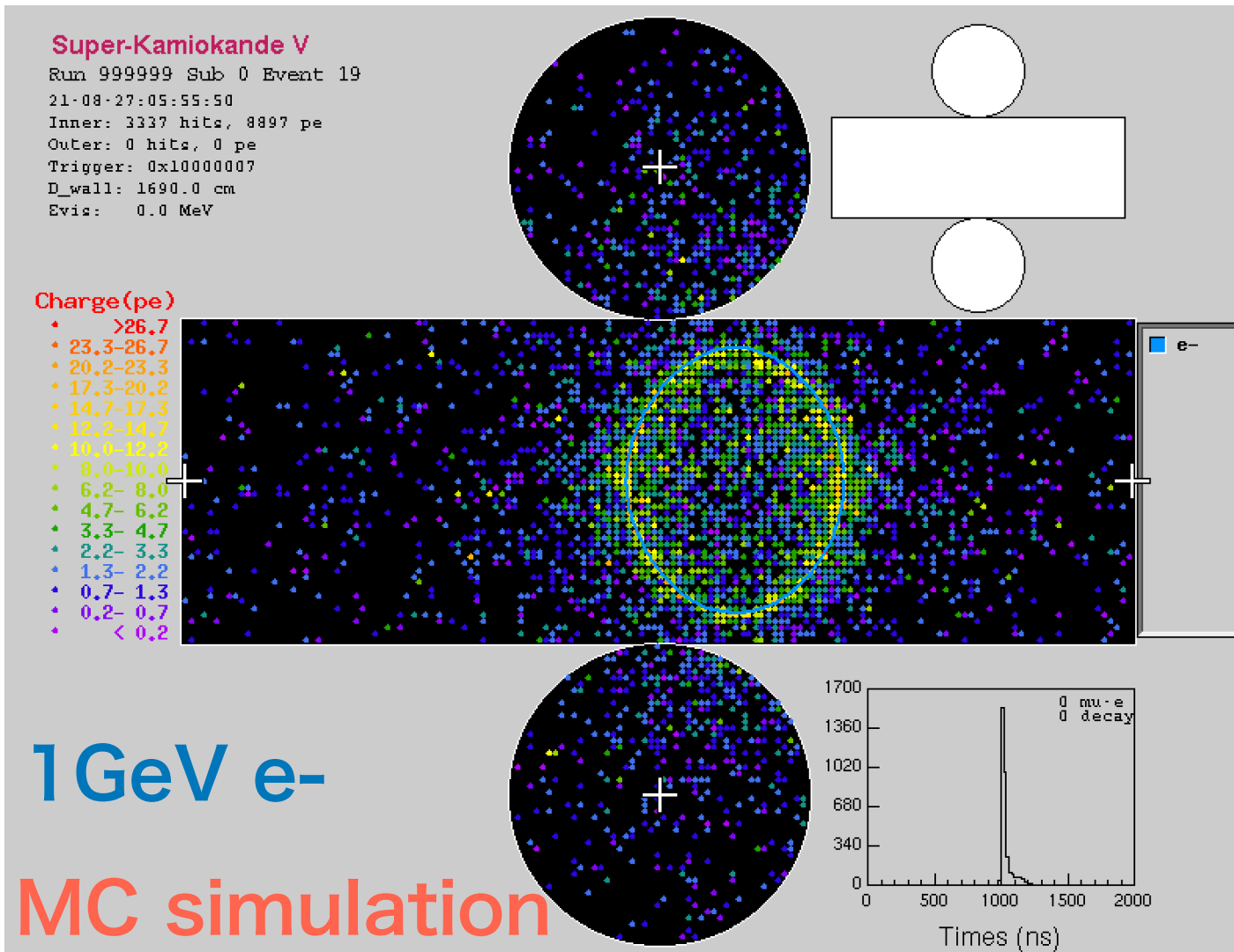
Super-Kamiokande



- World largest water Cherenkov detector [1]
- 50 kton water tank
 - ▶ 1996 ~ 2020: Ultra pure water
 - ▶ 2020 ~ : Gadolinium loaded water (SK-Gd [2])
- Detector
 - ▶ ID: 11,129 20-inch PMT
→ Event reconstruction using Timing and Charge
 - ▶ OD: 1,885 8-inch PMT
→ Cosmic-ray muon veto (~ 2 Hz)
- Sensitive energy
 - ▶ O(1) MeV ~ TeV

Multi purpose detector that covers a wide energy region

Photon attenuation in water



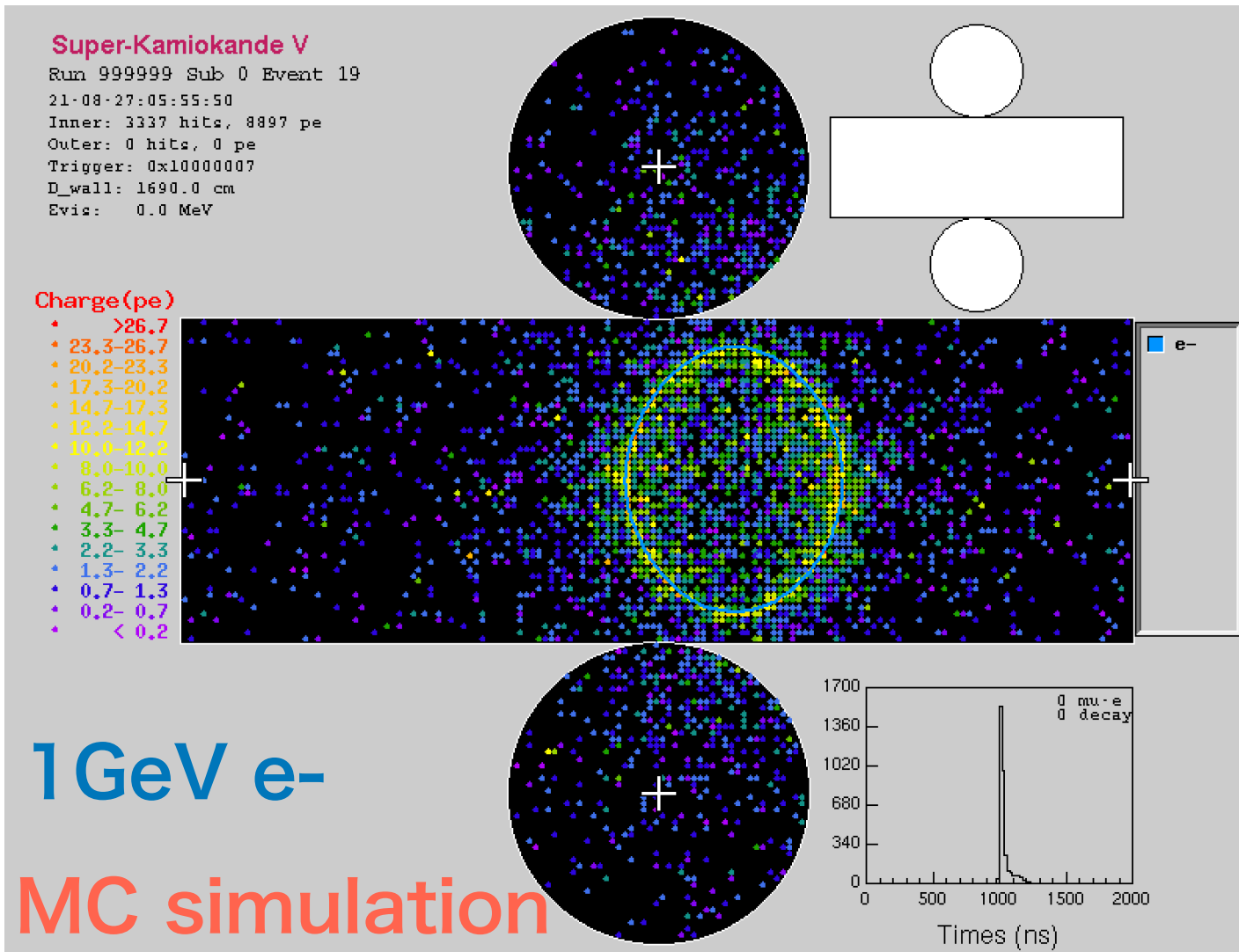
- Cherenkov photons are attenuated by electron or nucleus in water.
 - Absorption
 - Scattering
- Possible impact on analysis
 - GeV-scale
 - Cherenkov ring counting
 - Particle identification (μ or e)
 - Energy recon. using Charge
 - MeV-scale
 - Energy recon. using # of photons
 - Neutron detection using hit pattern

Important to understand and monitor the amount of such attenuation.

→ Water transparency “ $L(\lambda, t) [\text{m}]$ ”

$$I(\lambda) = I_0(\lambda) e^{-\frac{l}{L(\lambda, t)}}$$

Photon attenuation in water



Important to understand and monitor the amount of such attenuation.

→ Water transparency “ $L(\lambda, t) [\text{m}]$ ”

$L(\lambda, t)$ is being monitored for detector stability everyday.

$L(\lambda, t)$ is implemented into detector simulation as photon tracking.

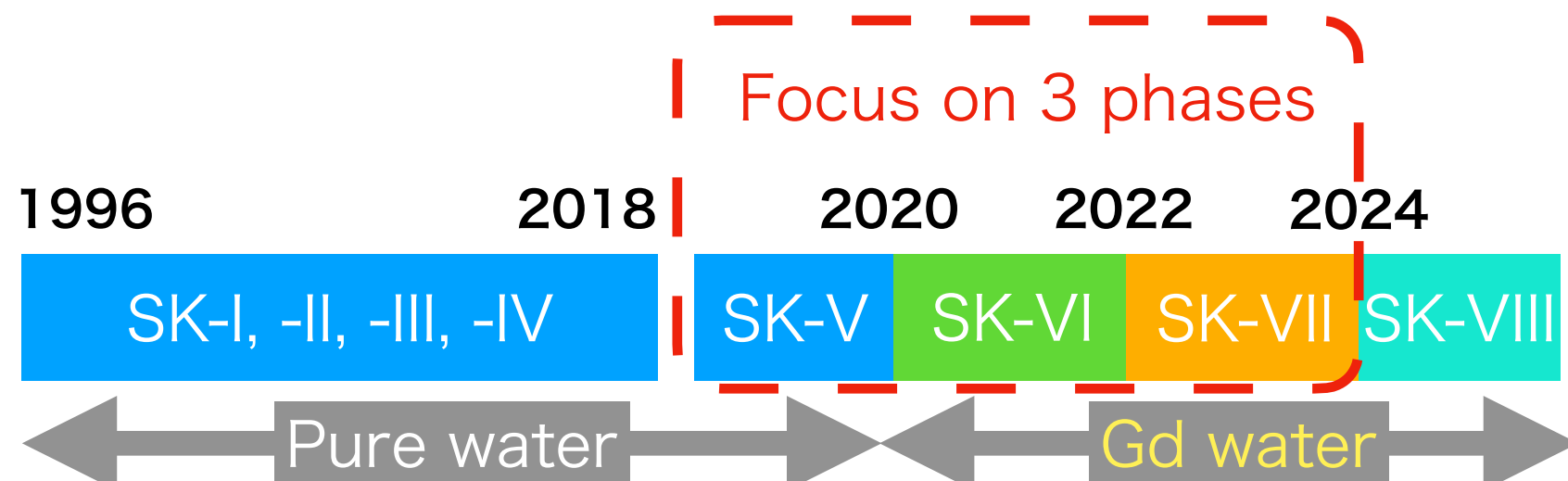
Photon attenuation in water

In this talk,

Measurement of wavelength-dependent $L(\lambda, t)$
and **Implementation** into detector simulation

Contents

- Optical laser system in SK detector
- SK detector simulation
 - ▶ Photon attenuation
- Analysis
 - ▶ PMT hit timing distribution
 - ▶ Extraction of absorption and scattering
- Results

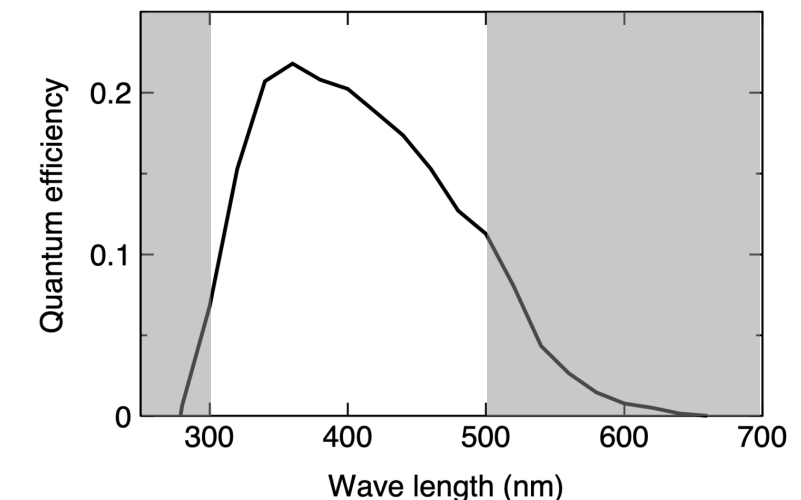


Optical laser system [3]

Calibration devices installed in SK detector (ID)

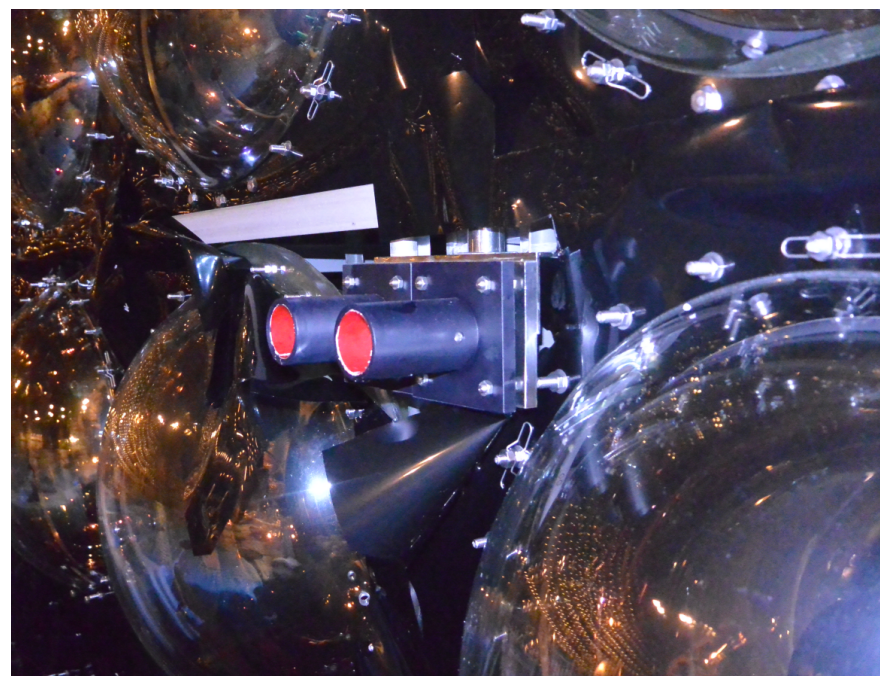
- ▶ 7 injectors
- ▶ 5 mono-wavelengths
 - 337, 375, 405, 445, 473 nm
 - Cover high Quantum Efficiency region of SK PMT.

Quantum Efficiency of PMT installed in Super-K

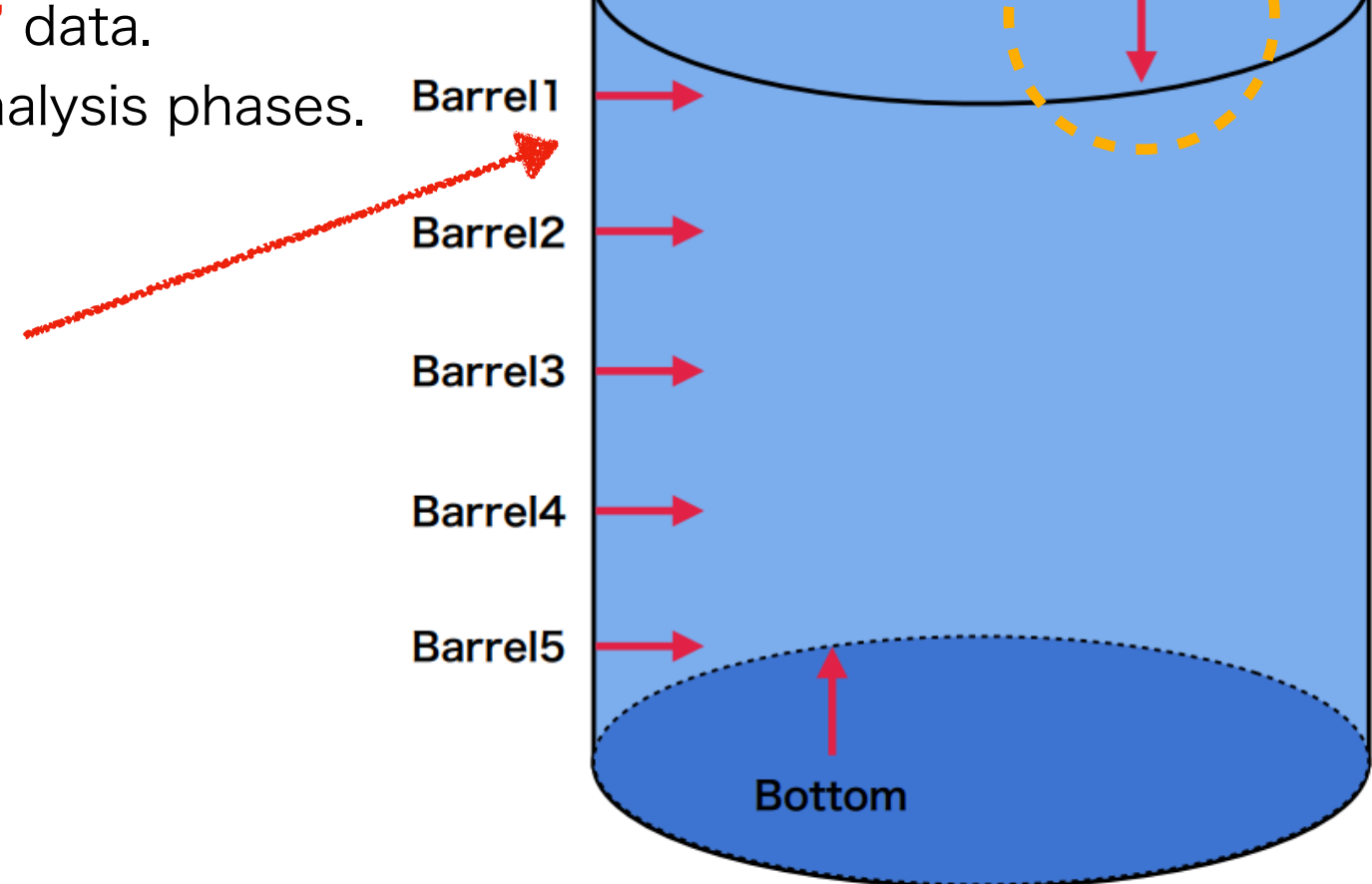


Automatic data taking

- ▶ Continuous data taking (parallel with physics run)
- ▶ Monitor the time variation of $L(\lambda, t)$.
- ▶ In this analysis, only use “Top laser” data.
 - Merged ~1 month data in each analysis phases.



Actual device photo



Detector simulation

- Detector Monte Carlo simulation
 - ▶ Geant4 based full detector simulation
 - ▶ Optical laser injector simulation is possible.
- Photon attenuation in simulation
 - ▶ 3 attenuation components

$$L(\lambda) = \frac{1}{\alpha_{abs}(\lambda) + \alpha_{sym}(\lambda) + \alpha_{asym}(\lambda)} \text{ [m]}$$

- ▶ Each component is depend on wavelength λ .
 - Empirical function [3]

Absorption

$$\alpha_{abs}(\lambda) = P_0 \times \frac{P_1}{\lambda^4} + P_0 \times P_2 \times 0.0279 \times \left(\frac{\lambda}{500}\right)^{P_3} \text{ [1/m]}$$

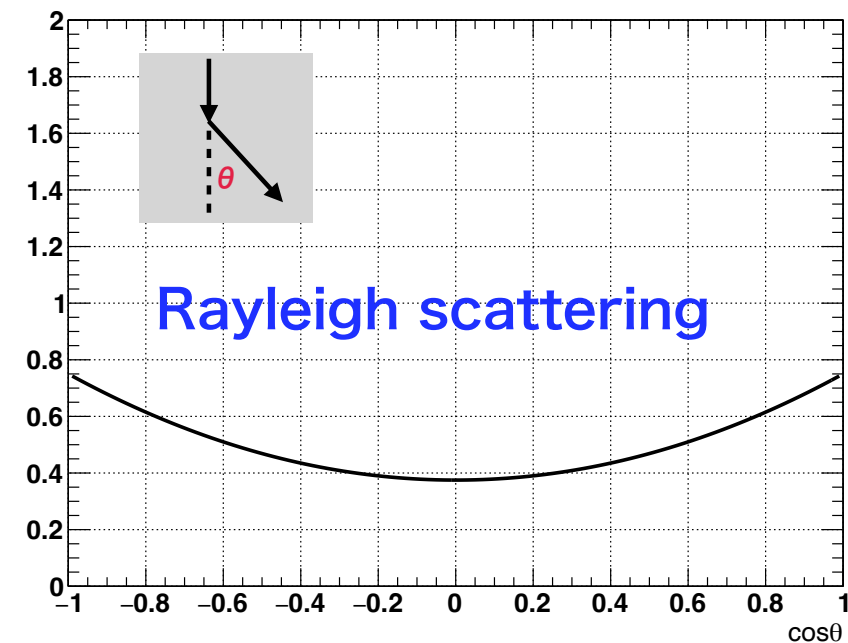
Rayleigh scattering (symmetric)

$$\alpha_{sym}(\lambda) = \frac{P_4}{\lambda^4} \times \left(1.0 + \frac{P_5}{\lambda^2}\right) \text{ [1/m]}$$

Mie scattering (asymmetric)

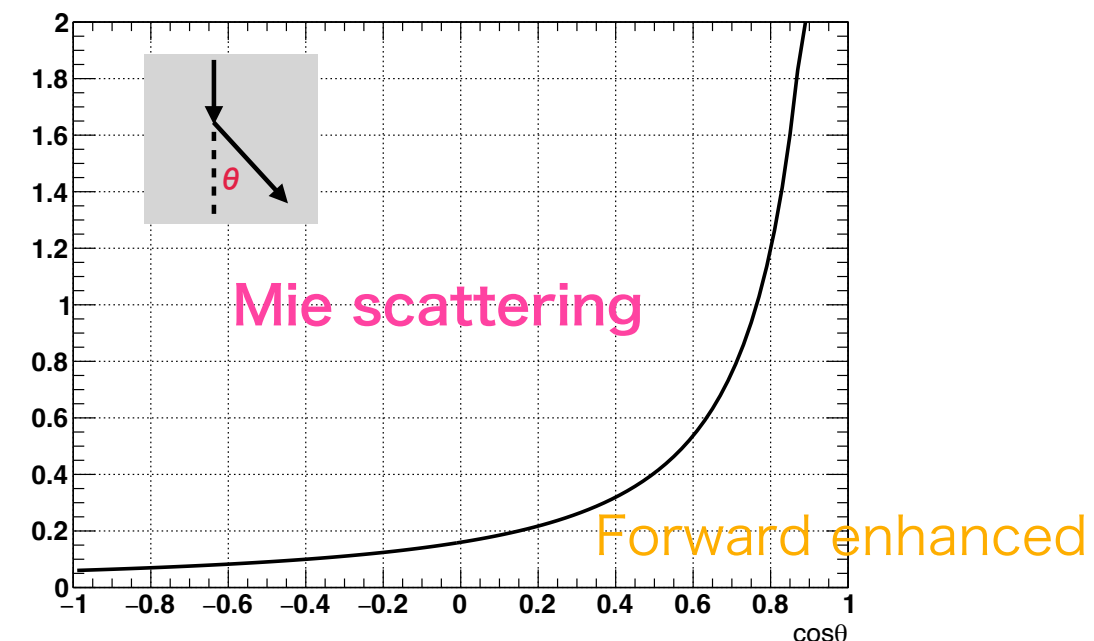
$$\alpha_{asym}(\lambda) = P_6 \times \left(1.0 + \frac{P_7}{\lambda^4} \times (\lambda - P_8)^2\right) \text{ [1/m]}$$

Scattering angular dist.



Backward

Forward

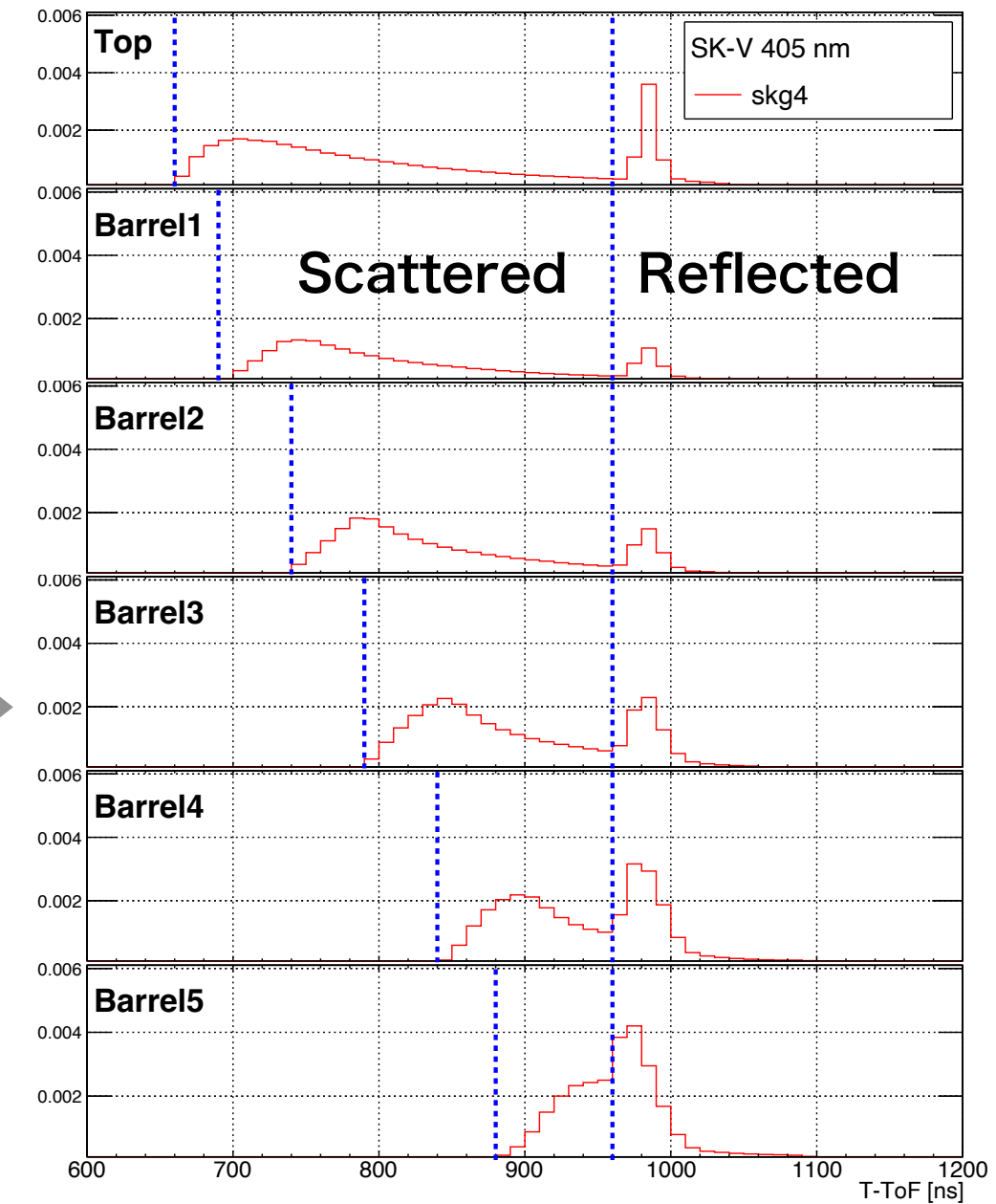
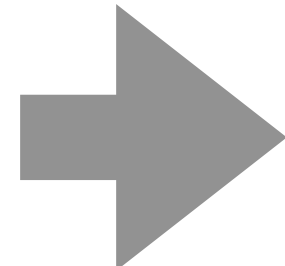
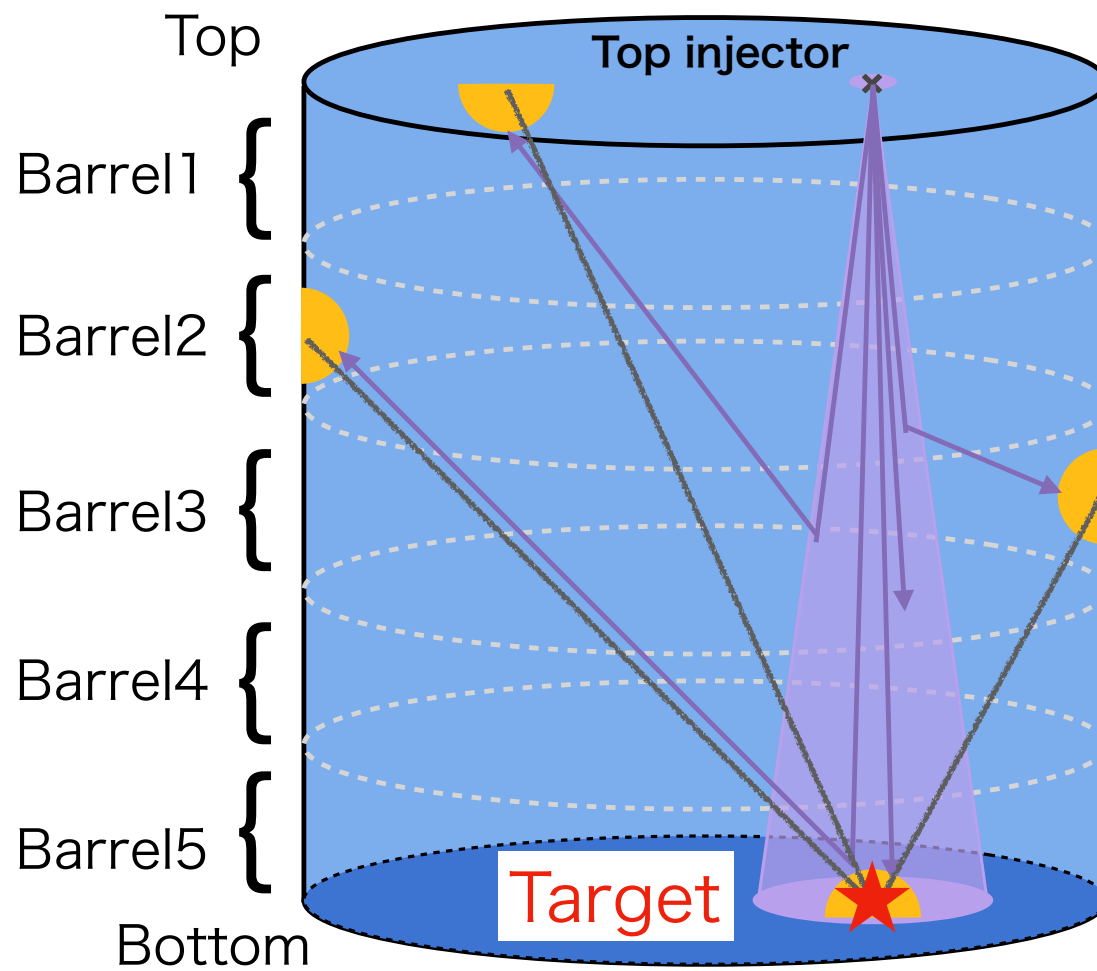


Optimize these functions by comparing the laser data and detector simulation.

Analysis ~ Hit timing distribution ~

8

- PMT hit timing distribution : Subtracted Time-of-flight
 - ToF : Distance from **the target (laser spot)** to the hit PMT
- PMT region (6 region)
 - 6 regions (Top + 5 Barrels)
 - **Top** : outside 2m from laser injector
 - **Barrel** : divide in detector height



Separate **scattered photon** and **reflected photon** (peak).
→ Absorption and scattering can be evaluated.

Analysis ~ Searching best-fit ~

MC production

- Changed $\alpha_{abs}(\lambda)$, $\alpha_{sym}(\lambda)$, $\alpha_{asym}(\lambda)$ independently
- 3D scanning

Normalization of timing distribution

- Total charge from laser

Chi-square definition

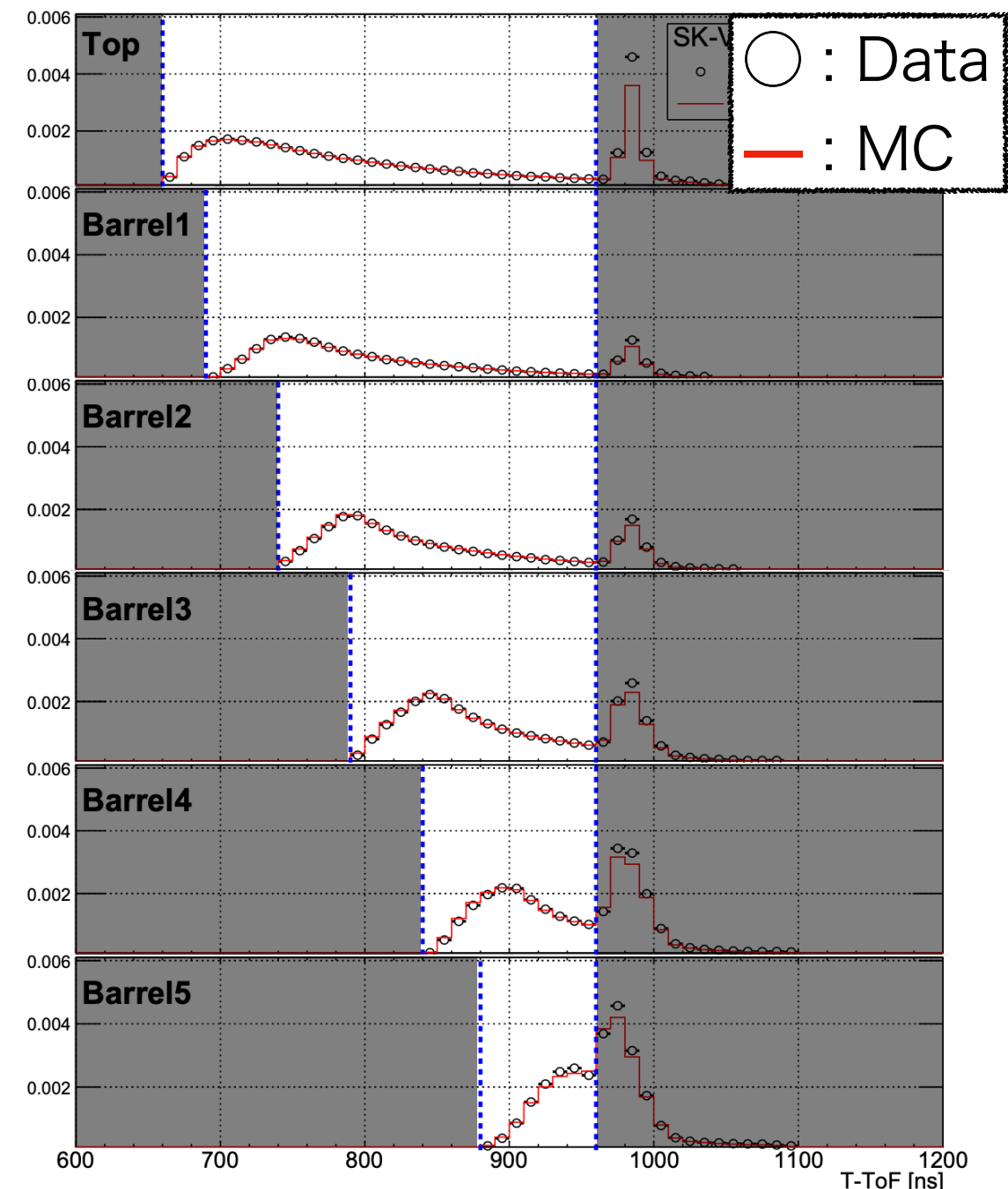
- Scattered region (between blue dot line)

$$\chi^2 = \sum_i^{\text{Nbins}} \frac{(N_i^{\text{Data}} - N_i^{\text{MC}})^2}{(\sigma_i^{\text{Data}})^2 + (\sigma_i^{\text{MC}})^2}$$

Chi-square minimization

- Evaluate combined χ^2

$$\chi^2_{\text{combined}} = \frac{\chi^2_{\text{Top}} + \chi^2_{B1} + \chi^2_{B2} + \chi^2_{B3} + \chi^2_{B4} + \chi^2_{B5}}{\text{Nbins}_{\text{Top}} + \text{Nbins}_{B1} + \text{Nbins}_{B2} + \text{Nbins}_{B3} + \text{Nbins}_{B4} + \text{Nbins}_{B5}}$$



Best-fit $\alpha_{abs}(\lambda)$, $\alpha_{sym}(\lambda)$, $\alpha_{asym}(\lambda)$ are determined at each wavelengths.

→ Repeat same analysis to 5 wavelengths.

Best-fit timing distribution (SK-V)



10

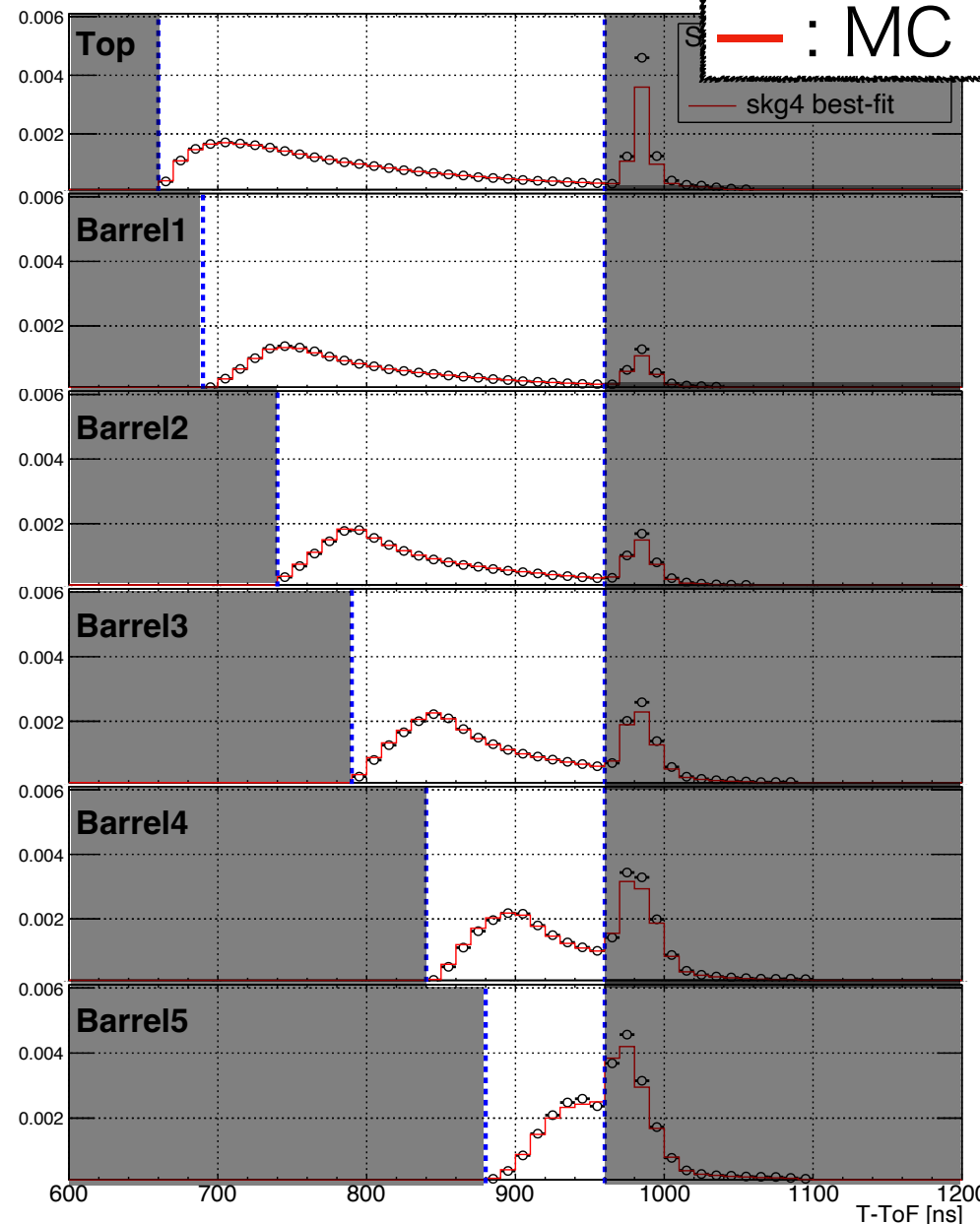
- Laser MC with best-fit absorption and scattering components

405nm

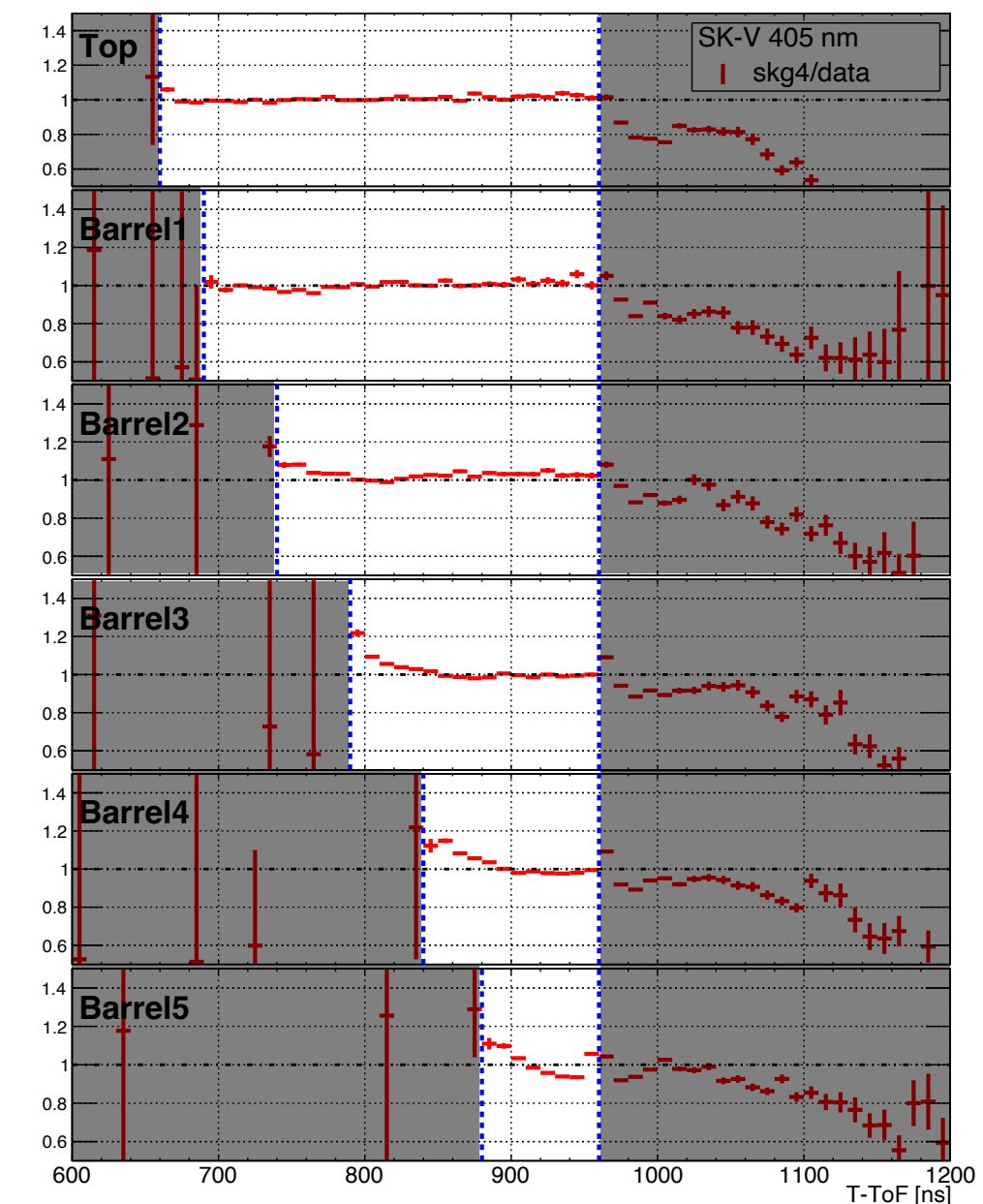
Overlay

○ : Data
— : MC
skg4 best-fit

Top
Barrel1
Barrel2
Barrel3
Barrel4
Barrel5



Ratio: MC/Data



Laser data and best-fit MC agree within < 10% level.

Best-fit timing distribution (SK-VI)



11

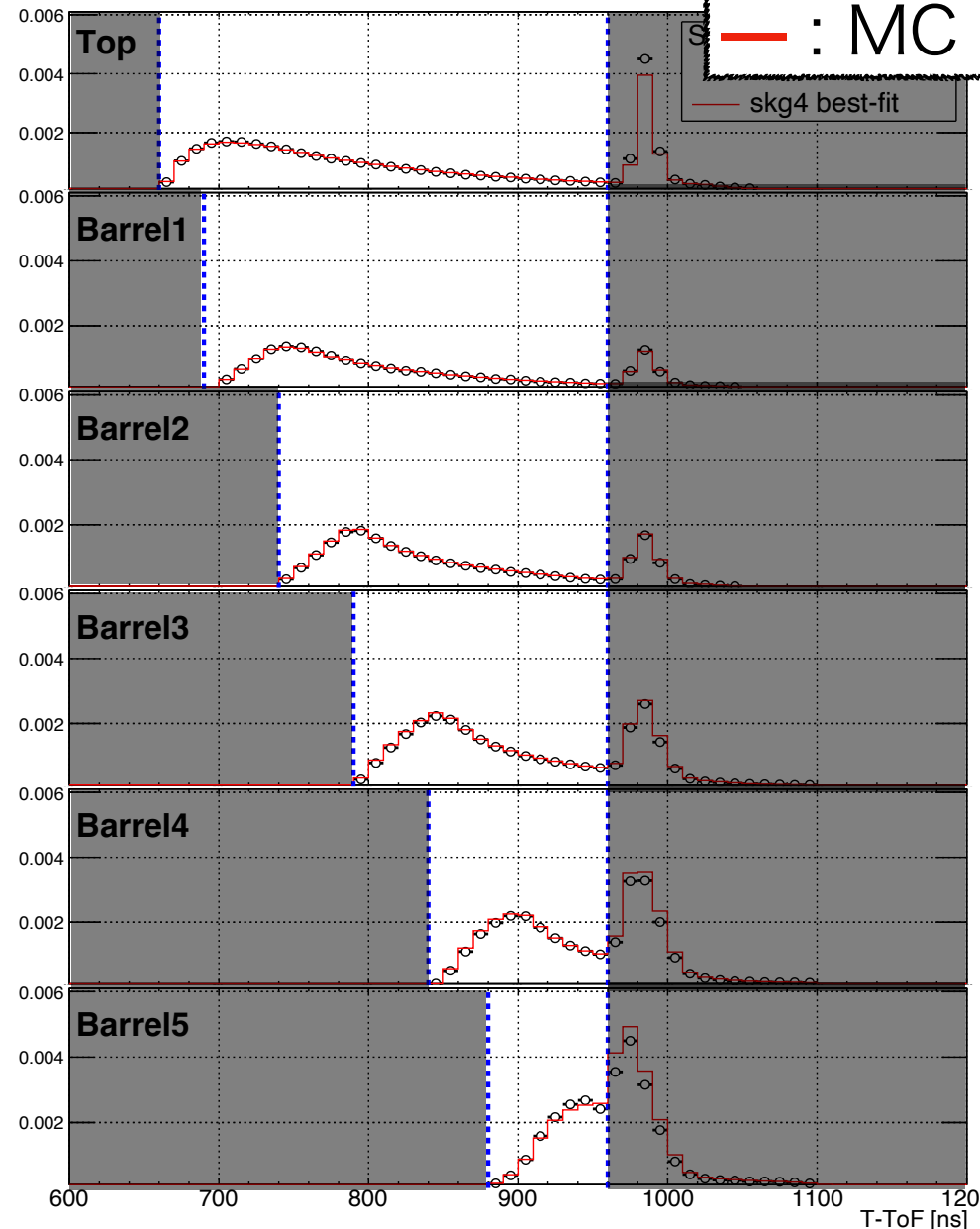
- Laser MC with best-fit absorption and scattering components

405nm

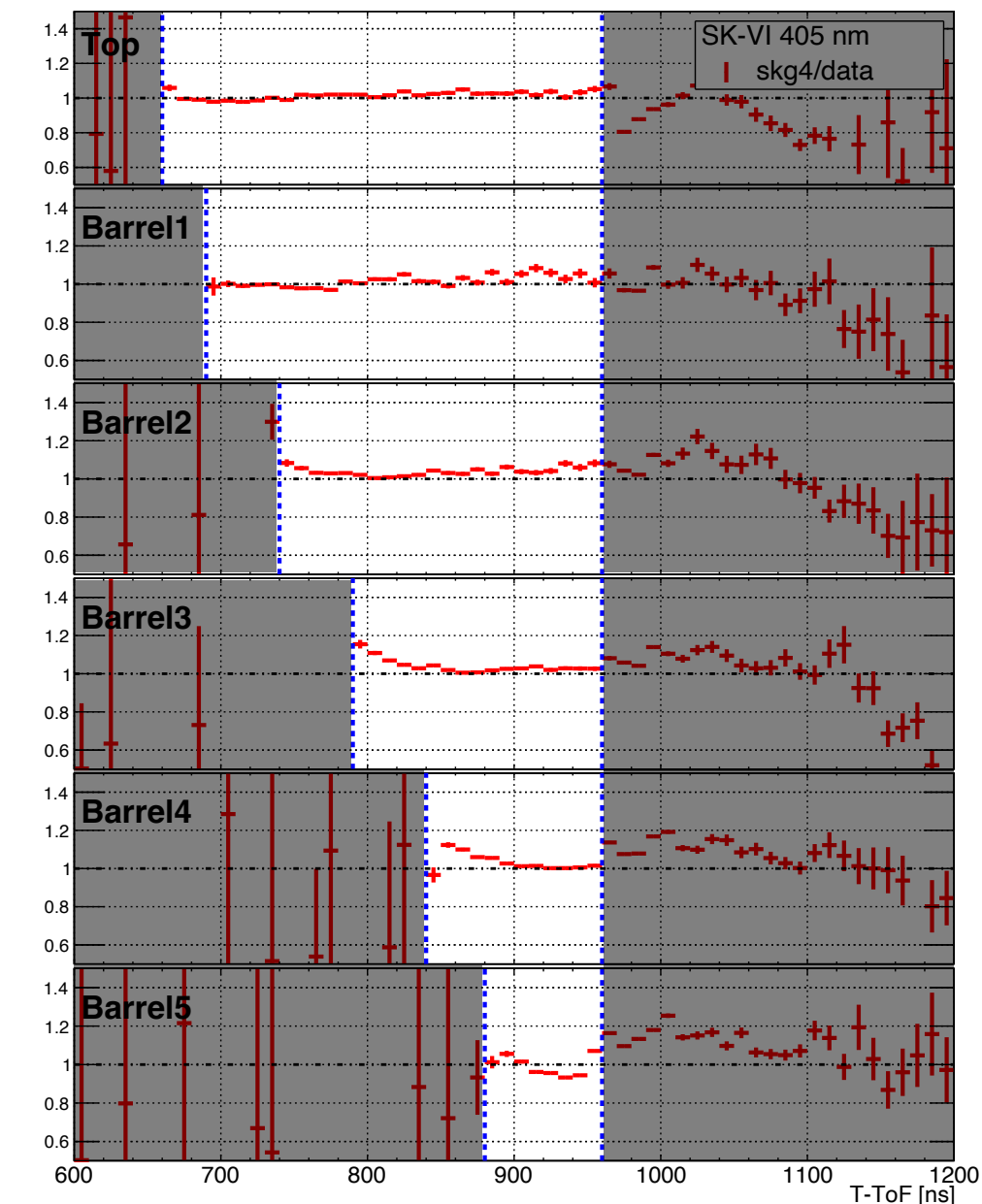
Overlay

○ : Data
— : MC
skg4 best-fit

Top
Barrel1
Barrel2
Barrel3
Barrel4
Barrel5



Ratio: MC/Data



Laser data and best-fit MC agree within < 10% level.

Best-fit timing distribution (SK-VII)

12

- Laser MC with best-fit absorption and scattering components

405nm

Overlay

○ : Data
— : MC
skg4 best-fit

Top

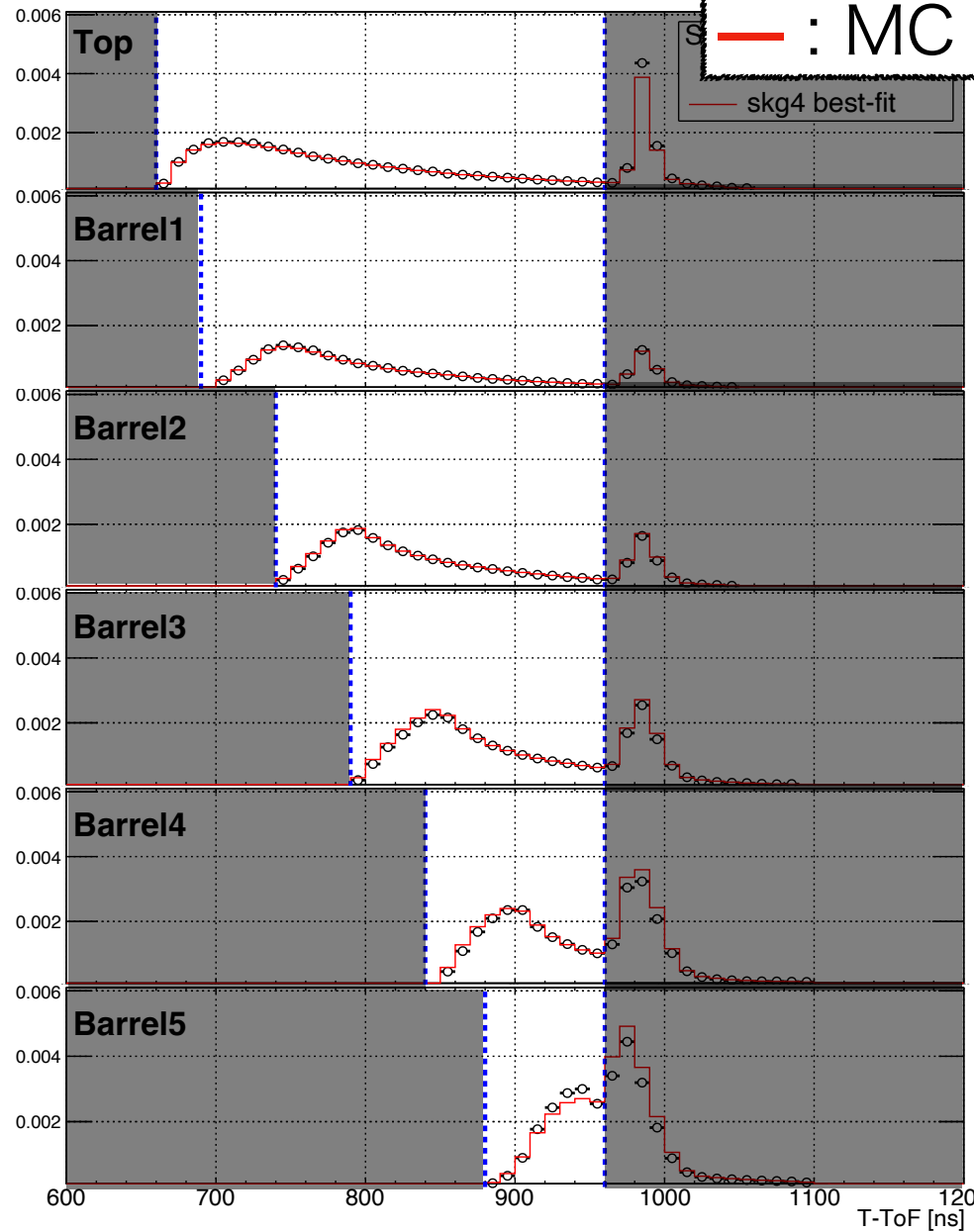
Barrel1

Barrel2

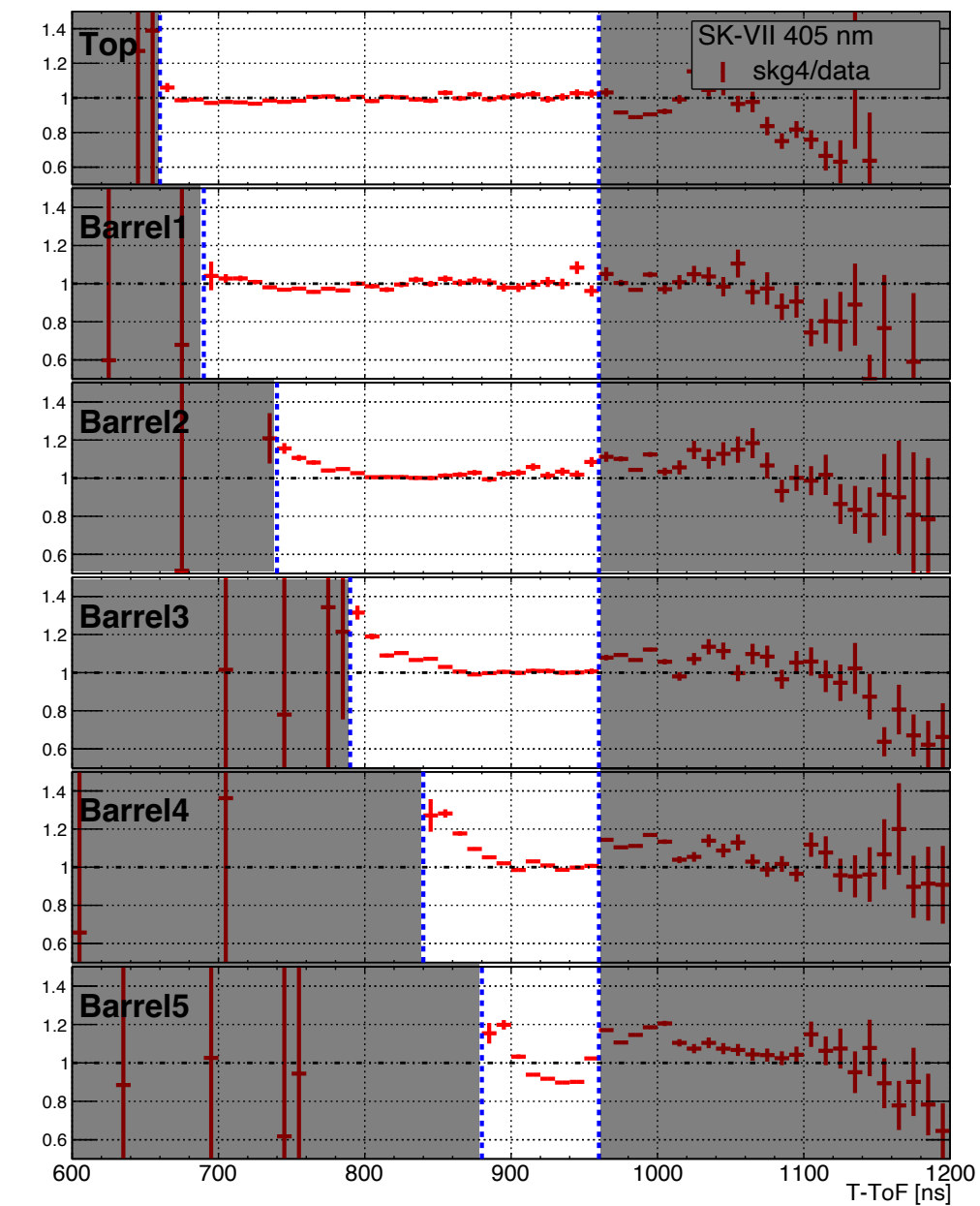
Barrel3

Barrel4

Barrel5



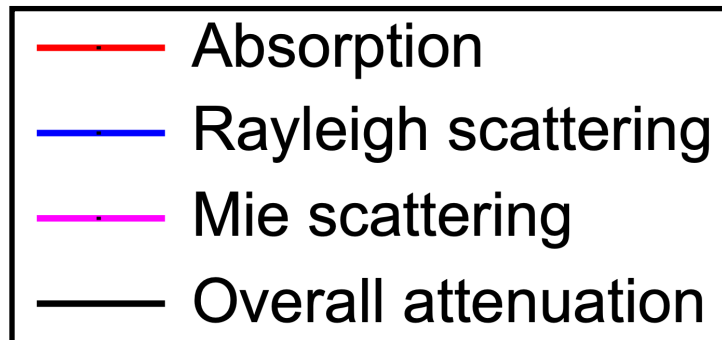
Ratio: MC/Data



Laser data and best-fit MC agree within < 10% level.

Results

- Fitting best-fit attenuation components



Absorption

$$\alpha_{abs}(\lambda) = P_0 \times \frac{P_1}{\lambda^4} + P_0 \times P_2 \times 0.0279 \times \left(\frac{\lambda}{500}\right)^{P_3} [1/m]$$

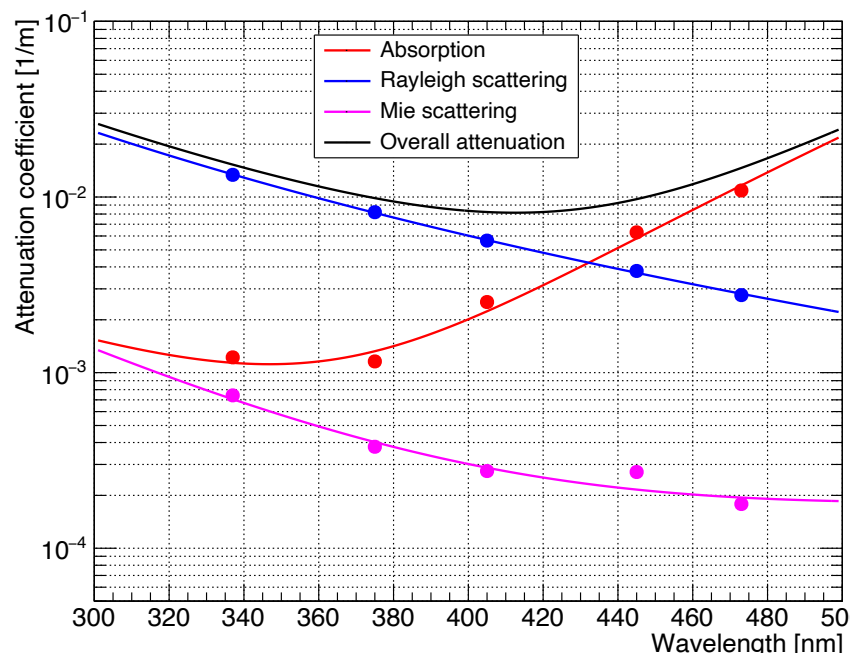
Rayleigh scattering (symmetric)

$$\alpha_{sym}(\lambda) = \frac{P_4}{\lambda^4} \times (1.0 + \frac{P_5}{\lambda^2}) [1/m]$$

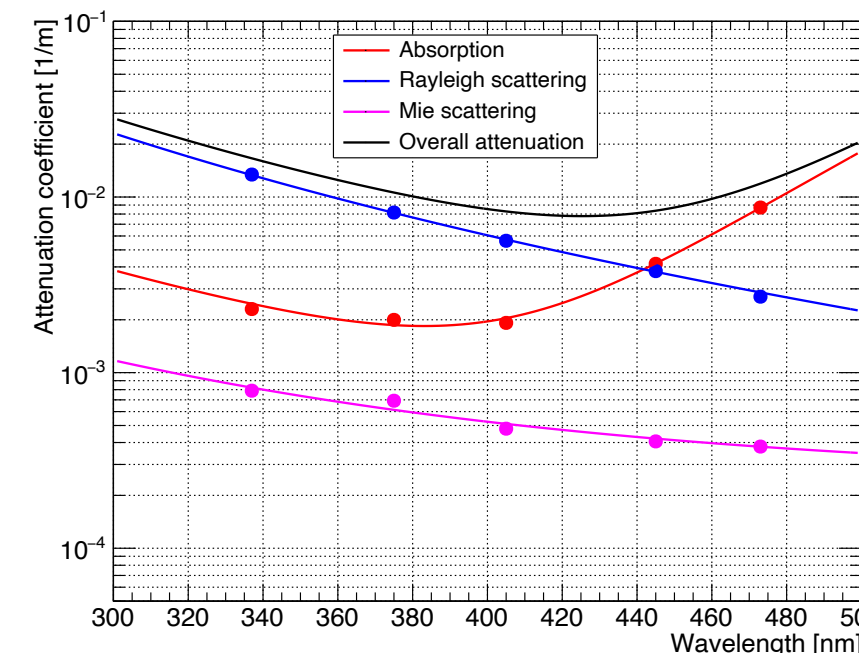
Mie scattering (asymmetric)

$$\alpha_{asym}(\lambda) = P_6 \times (1.0 + \frac{P_7}{\lambda^4} \times (\lambda - P_8)^2) [1/m]$$

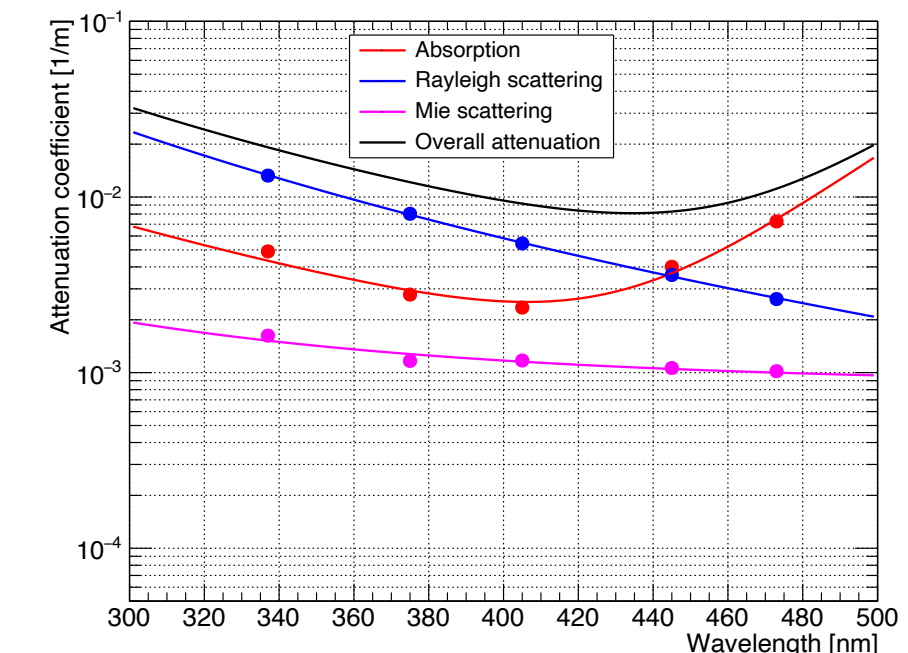
SK-V



SK-VI



SK-VII



Water transparency over 100m (10^{-2} [1/m]) is achieved in high QE region of SK PMT.

In detector simulation, these fitted functions are implemented for Cherenkov photon tracking.

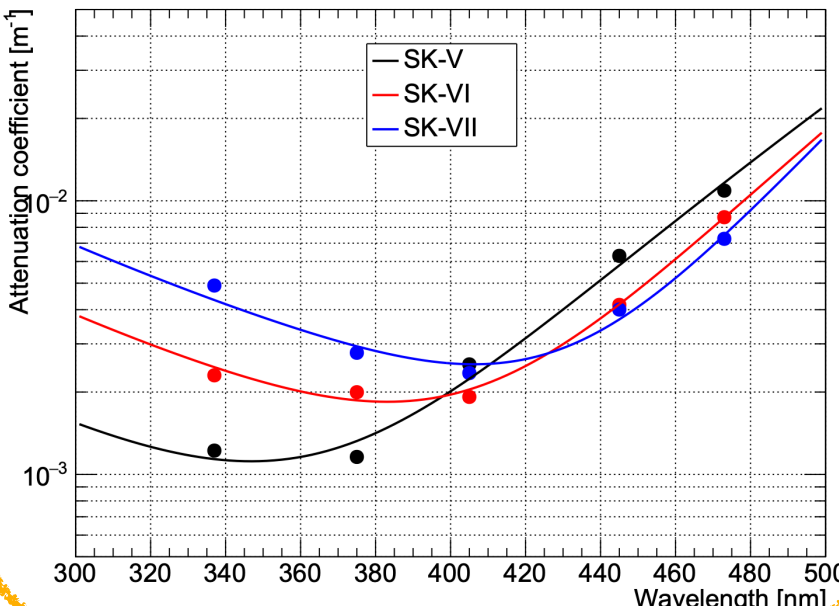
→ Physics analysis

Comparison among phases

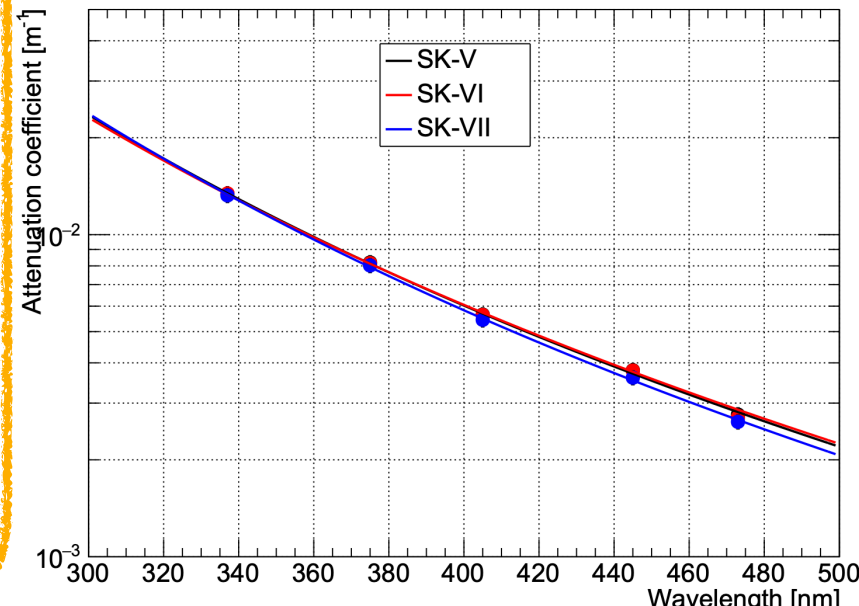
- SK-V
- SK-VI
- SK-VII

- Comparisons of each attenuation component.
- ▶ Some differences among phases

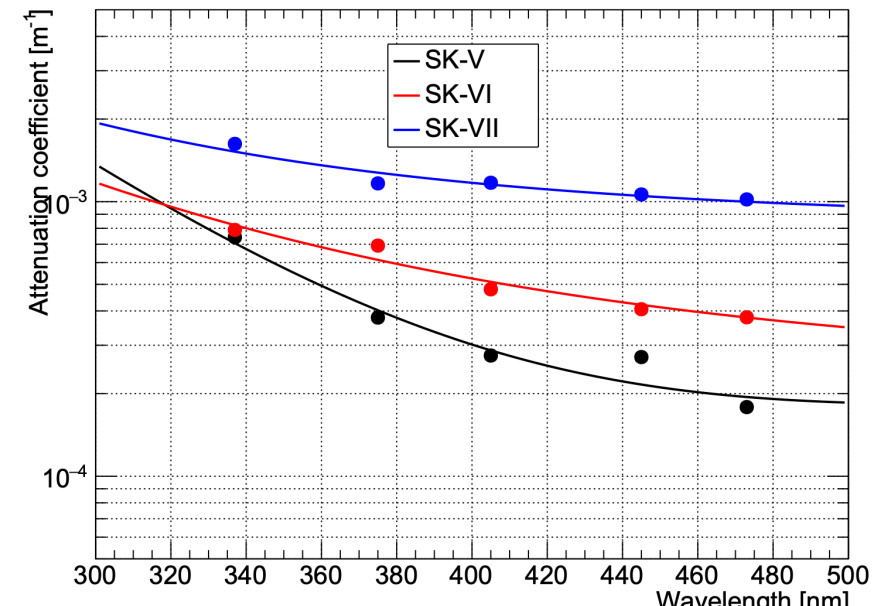
Absorption



Rayleigh



Mie



Absorption

- ▶ In short wavelength ($\lambda < 400\text{nm}$) , increasing with each phases.
→ There is a possibility that element other than Gd may be dissolved in water.
→ Now investigating water composition with company.

Mie scattering

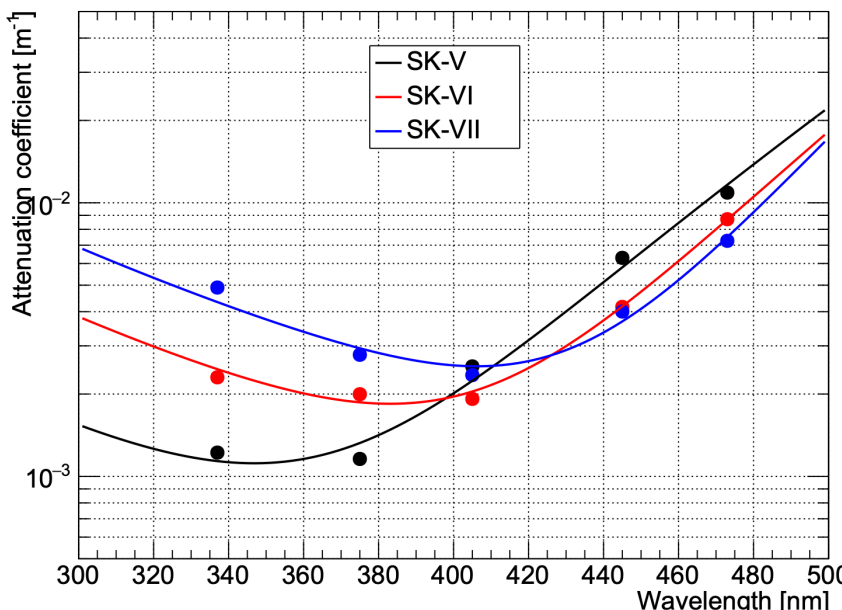
- ▶ Overall, increasing with each phases.
→ Possibility for increasing the large size impurities ($\sim \lambda$).
→ However, overall impact is small because 1 order smaller than Rayleigh scattering.

Comparison among phases

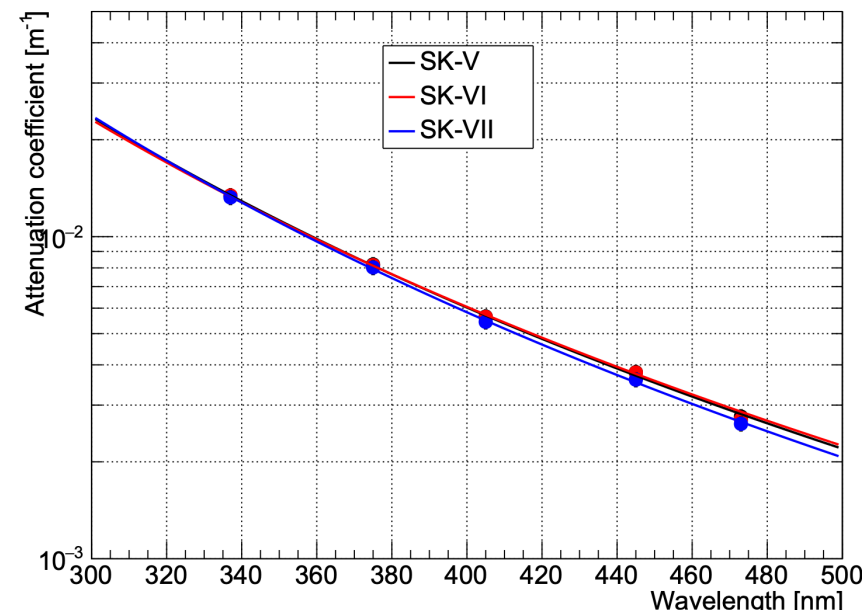
- SK-V
- SK-VI
- SK-VII

- Comparisons of each attenuation component.
- ▶ Some differences among phases

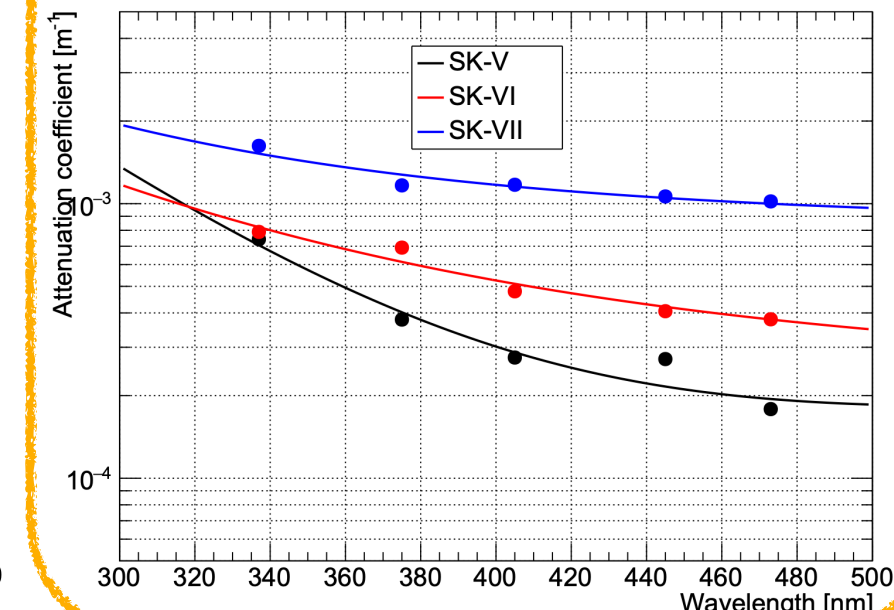
Absorption



Rayleigh



Mie



Absorption

- ▶ In short wavelength, increasing with each phases.
→ There is a possibility that element other than Gd may be dissolved in water.
→ Now investigating water composition with company.

Mie scattering

- ▶ Overall, increasing with each phases.
→ Possibility for increasing the large size impurities ($\sim \lambda$).
→ However, overall impact is small because 1 order smaller than Rayleigh scattering.

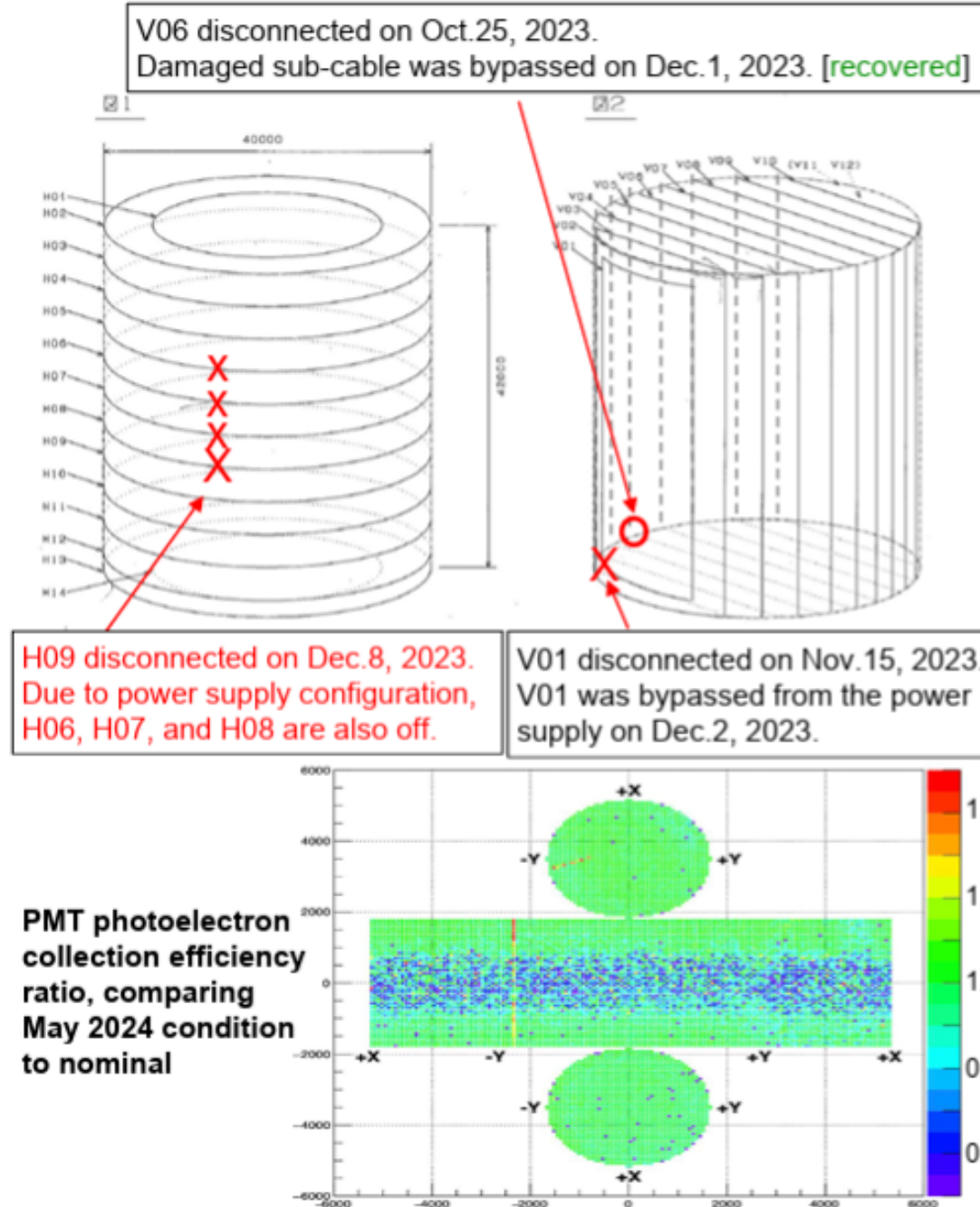
Summary

- Water transparency $L(\lambda, t)$ is crucial for Super-K physics analysis.
- $L(\lambda, t)$ is being monitored for detector stability everyday.
- In detector simulation, wavelength-dependent $L(\lambda, t)$ is implemented.
 - ▶ Optical laser data in 5 mono-wavelengths
 - ▶ χ^2 calculated using timing distribution in divided PMT region.
 - Water transparency over 100m is achieved in high Quantum Efficiency region of Super-K PMT.
 - Laser data and best-fit MC are agreed within 10% level in each analysis.
 - Best-fit functions are implemented into detector simulation and used in physics analysis.
- In comparison among 3 phases, there are differences in attenuation coefficient.
 - ▶ Absorption ($\lambda < 400$ nm)
 - ▶ Mie scattering
 - Now investigating water composition with company.
- We will perform measurement in SK-VIII with same analysis method.
- Additionally, we are considering a new measurement of the vertical dependence of $L(\lambda, t)$ using horizontal laser data.

Supplement

SK-VIII (from Sep. 2024)

SK's geomagnetic compensation coil problems and countermeasures

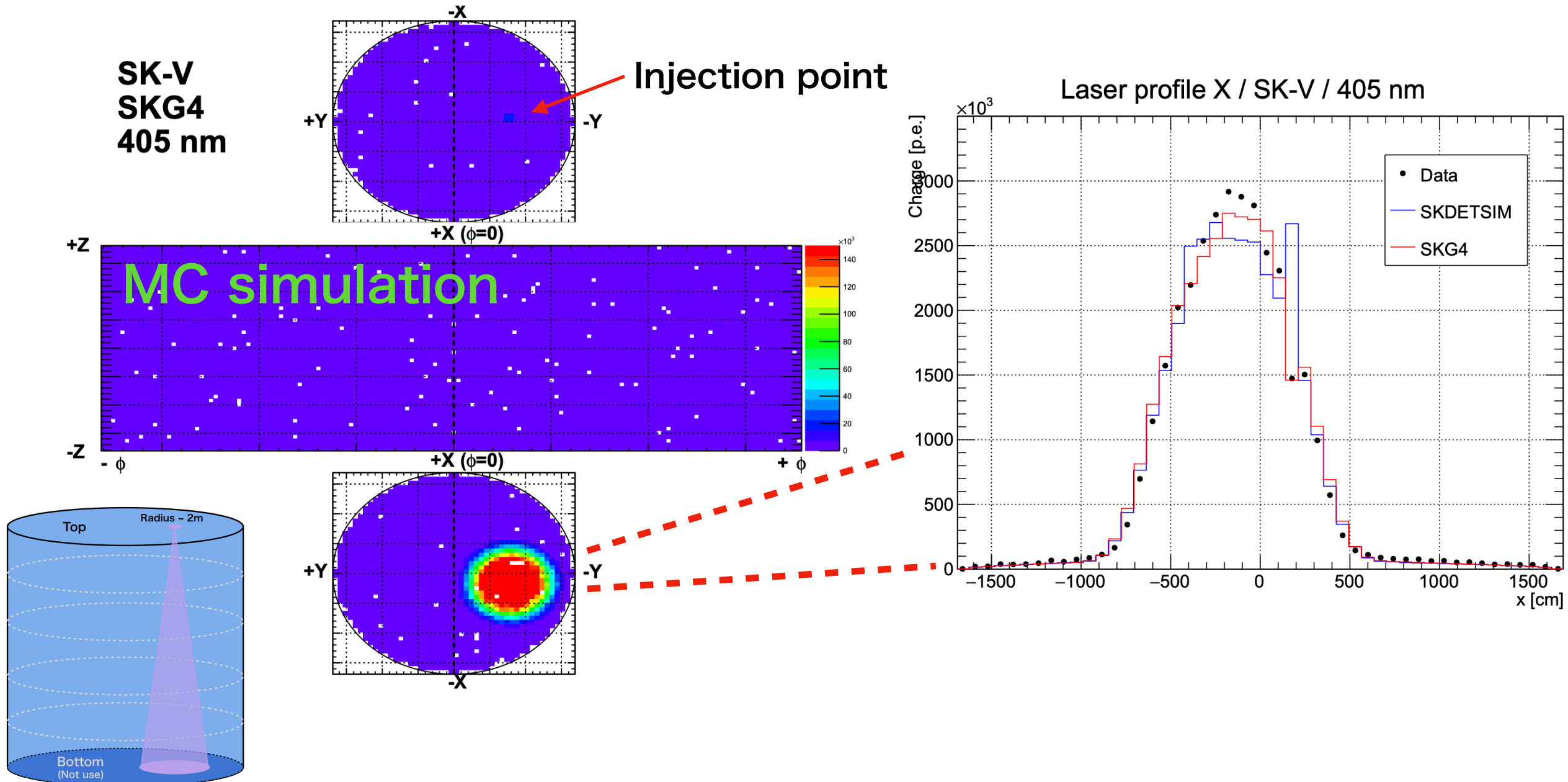


- SK geomagnetic compensation coil cables have failed in three locations.
 - At two of locations, part of the coil was successfully bypassed to restore functionality. The other location is entirely underwater, resulting in the entire cable group being turned off.
 - A 10-20% decrease in collection efficiency is observed for about 20% of PMTs in the barrel.
 - Efficiency for detecting neutron capture on Gd has also decreased by about 3%.
 - The physics impact can be compensated by calibration and simulation.
 - The likely cause is corrosion of wire connections due to ionized water seeping in under heat shrink insulation.
 - SK plans to install six new horizontal coils in summer 2024 to restore the geomagnetic field cancellation.

Compensation coil installing work was done in Aug. 2024.
After that, we started new observation phase “SK-VIII”.

Optical laser simulation

- Optical photon injection
- Implemented direction and divergence calculated from laser data.



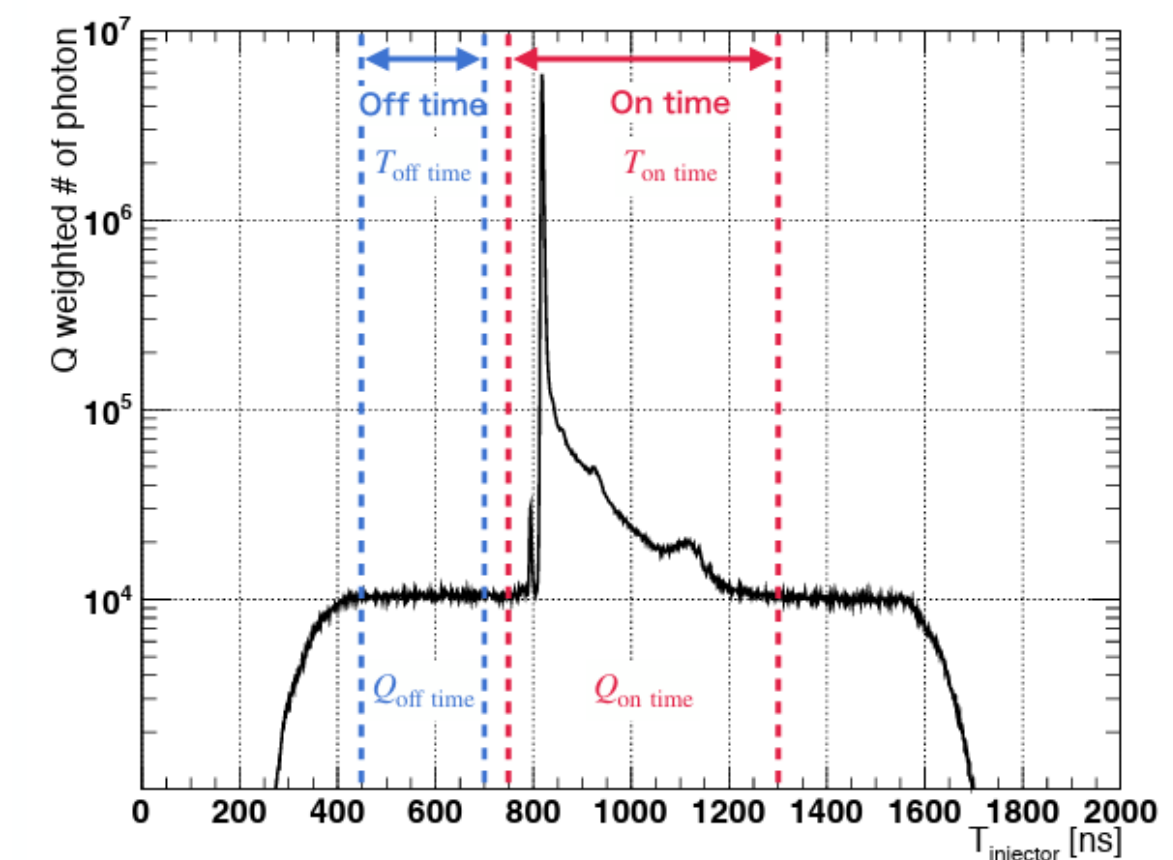
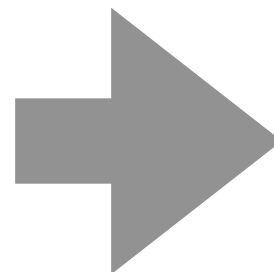
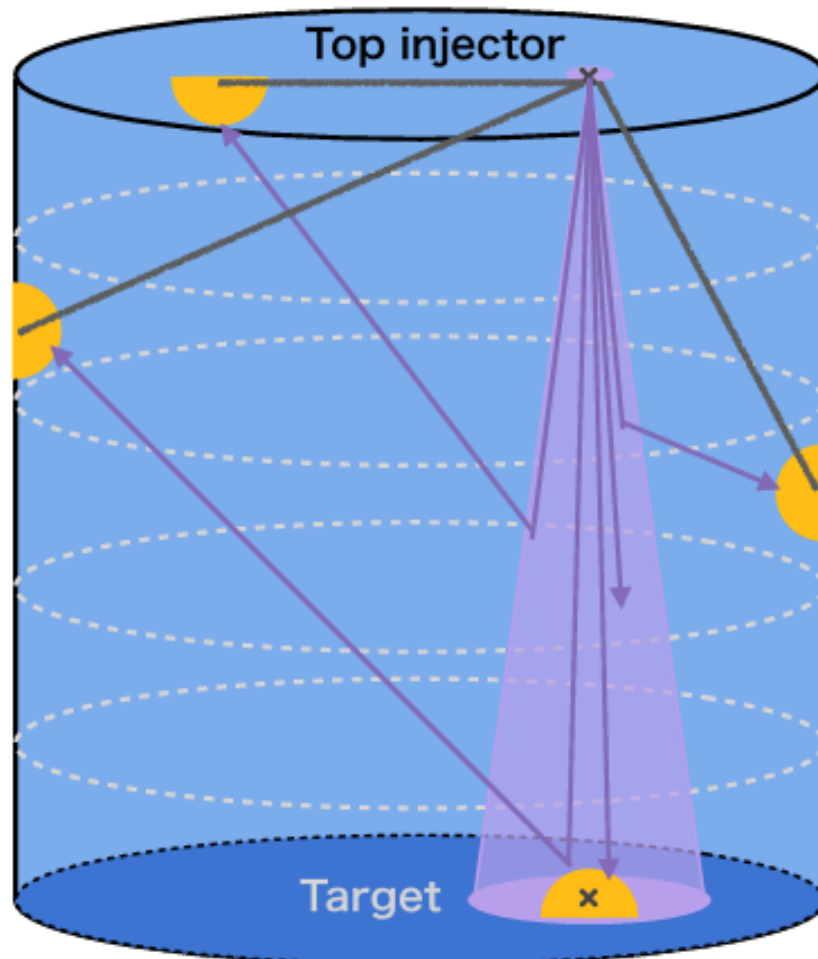
The topology of the laser event is reproduced in the simulations

Analysis ~ Normalization ~

- Normalization factor

- Total charge from laser
- Timing distribution (T-ToF)
 - Distance from laser injector
 - Include direct light

$$Q_{\text{laser}} = Q_{\text{on time}} - \frac{Q_{\text{off time}}}{T_{\text{off time}}} \times T_{\text{on time}}$$



Impact for timing distribution

Absorption

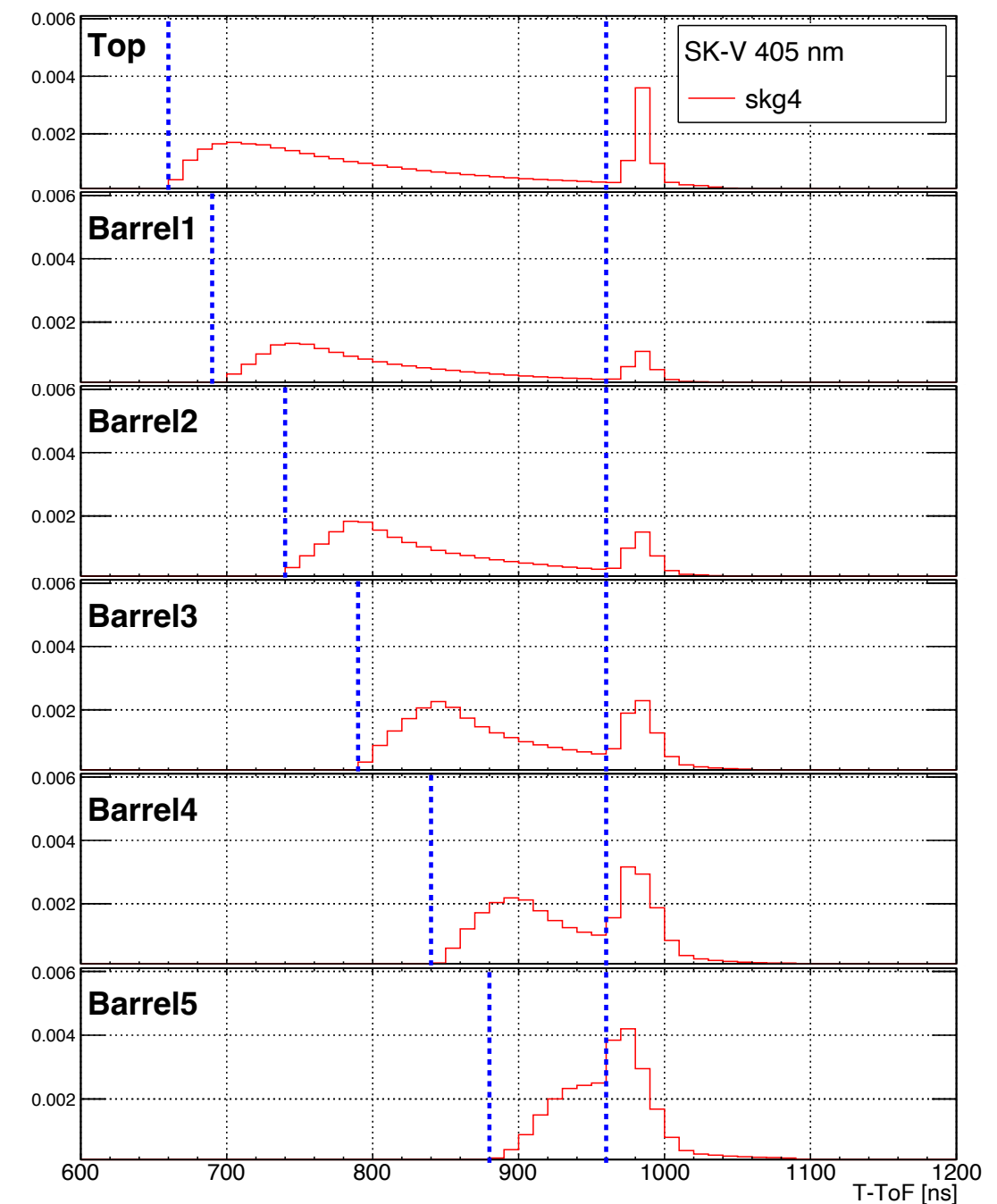
- ▶ This affects late hits in the scattering region.
- ▶ The effect of absorption is visible due to the long flight distance.

Raigh scattering

- ▶ It has the largest contribution and affects the entire scattering region.

Mie scattering

- ▶ Due to the strong forward scattering, this only affects the time distribution of the PMT forward from the laser. (Barrel3, 4, 5)
- ▶ In particular, it affects early hits in the scattering region.



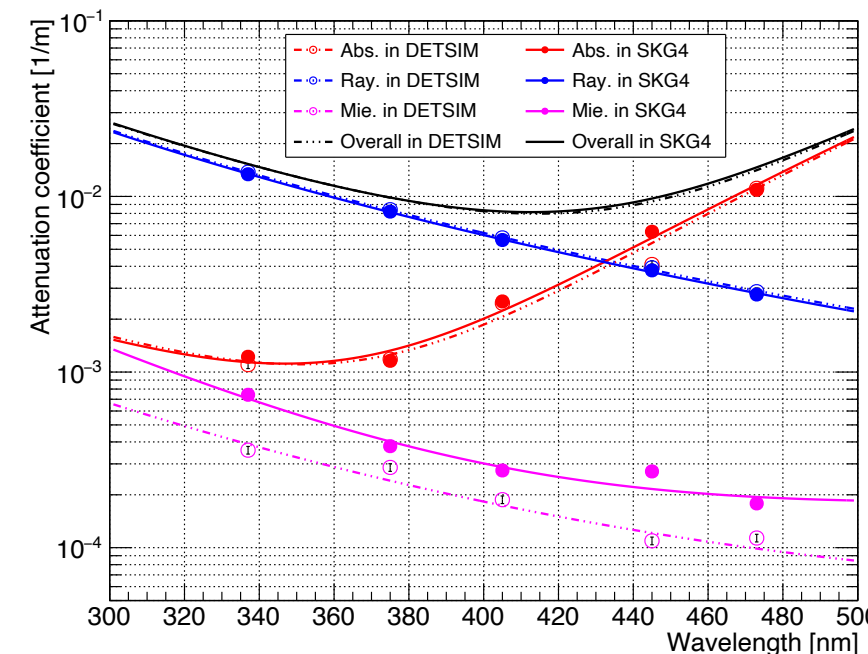
Comparison of MCs

22

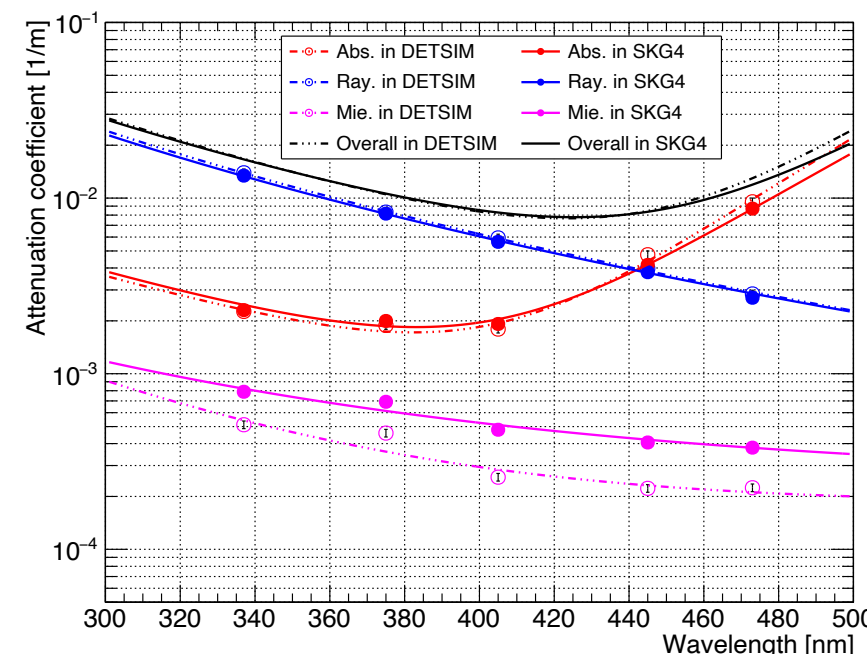
- Attenuation components and these functions are same between 2 MCs

	SKDETSIM	SKG4
Tool	GEANT3	Geant4
Language	FORTRAN	C++

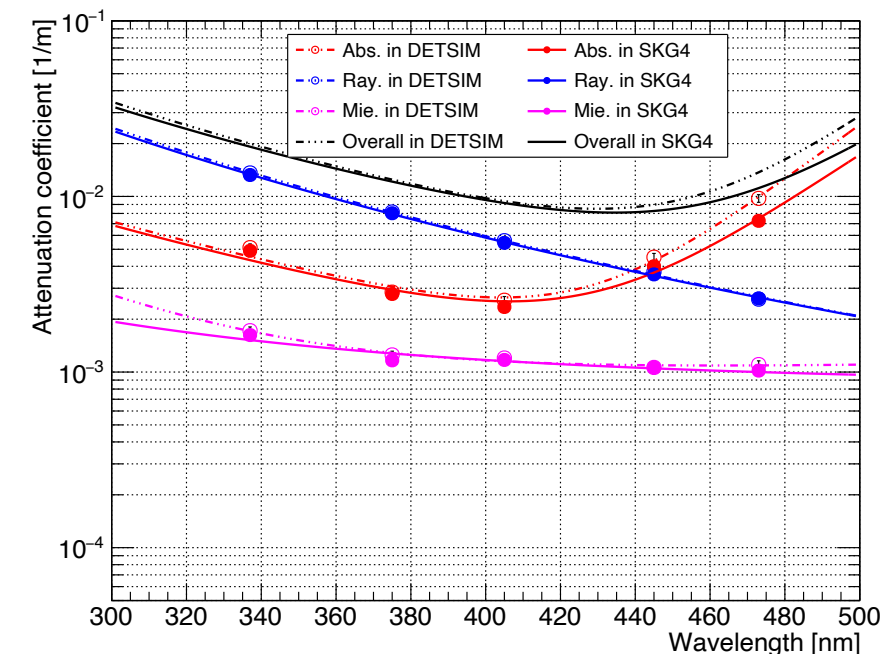
SK-V



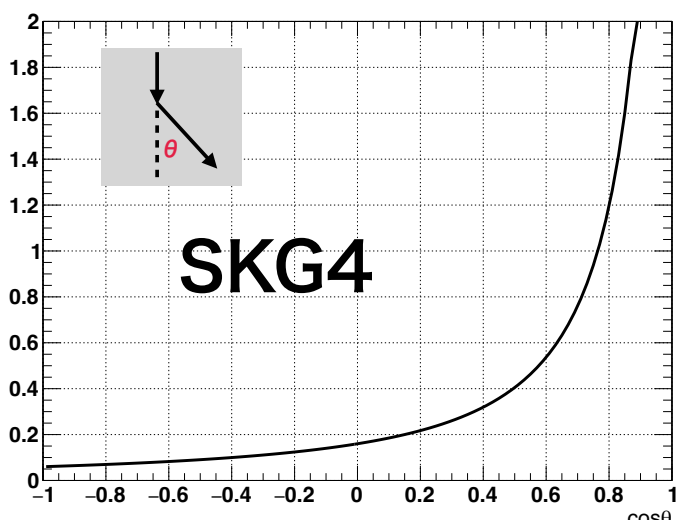
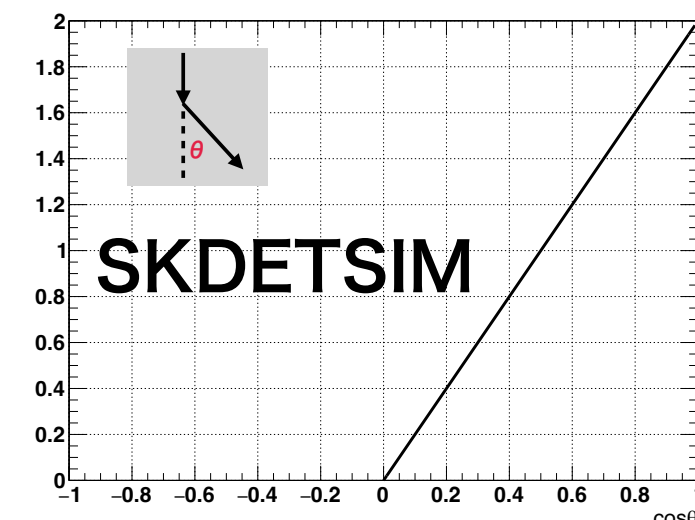
SK-VI



SK-VII



- Absorption and Rayleigh scattering are almost same.
- Mie scattering is different.
→ Scattering angular distribution
- From SK-VII, modeling is unified.

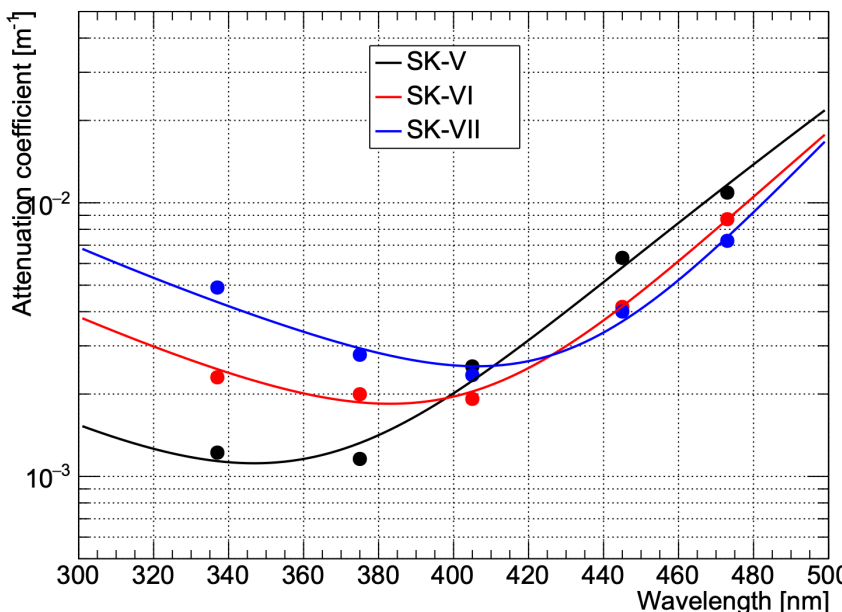


Comparison among phases

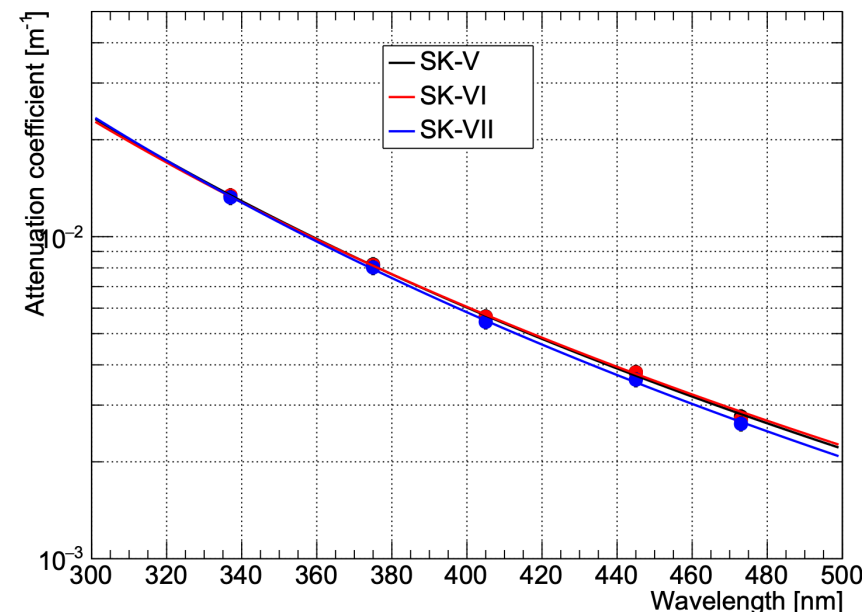
- SK-V
- SK-VI
- SK-VII

- Comparisons of each attenuation component.
- ▶ Some differences among phases

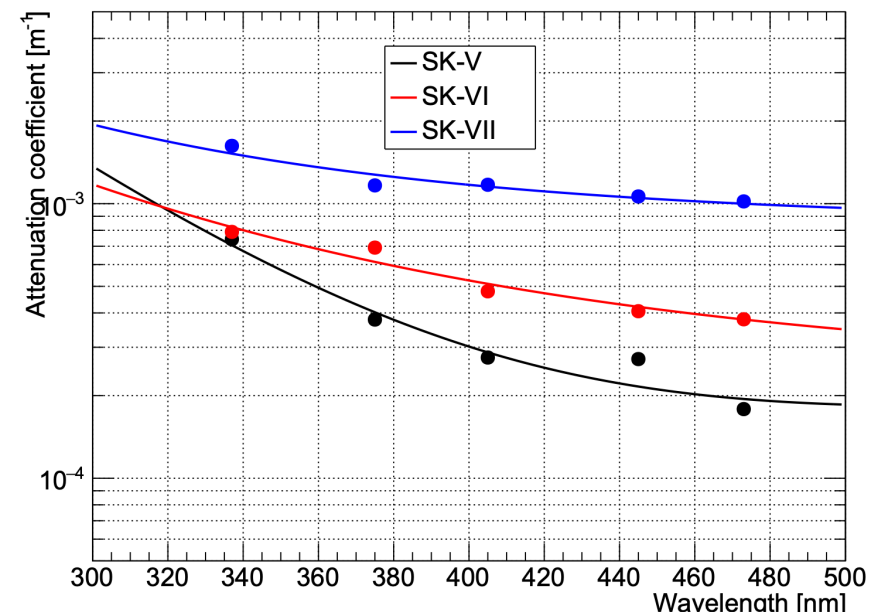
Absorption



Rayleigh



Mie



Absorption

- ▶ In short wavelength, increasing with each phases.
→ There is a possibility that element other than Gd may be dissolved in water.
→ Now investigating water composition with company.

Mie scattering

- ▶ Overall, increasing with each phases.
→ Possibility for increasing the large size impurities ($\sim \lambda$).
→ However, overall impact is small because 1 order smaller than Rayleigh scattering.

Calibration in SK-IV

● NIM A 737 (2014) 253-272

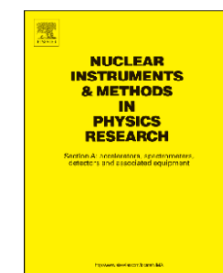
Nuclear Instruments and Methods in Physics Research A 737 (2014) 253–272



Contents lists available at ScienceDirect

Nuclear Instruments and Methods in Physics Research A

journal homepage: www.elsevier.com/locate/nima



Calibration of the Super-Kamiokande detector



K. Abe^a, Y. Hayato^{a,ad}, T. Iida^{a,1}, K. Iyogi^a, J. Kameda^a, Y. Kishimoto^{a,ad}, Y. Koshio^{a,*},
 Ll. Martí^{a,2}, M. Miura^a, S. Moriyama^{a,ad}, M. Nakahata^{a,ad}, Y. Nakano^a, S. Nakayama^a,
 Y. Obayashi^{a,3}, H. Sekiya^a, M. Shiozawa^{a,ad}, Y. Suzuki^{a,ad}, A. Takeda^a, Y. Takenaga^a,
 H. Tanaka^a, T. Tomura^a, K. Ueno^{a,4}, R.A. Wendell^a, T. Yokozawa^{a,5}, T.J. Irvine^b, H. Kaji^b,
 T. Kajita^{b,ad}, K. Kaneyuki^{b,ad,11}, K.P. Lee^b, Y. Nishimura^b, K. Okumura^b, T. McLachlan^b,
 L. Labarga^c, E. Kearns^{e,ad}, J.L. Raaf^e, J.L. Stone^{e,ad}, L.R. Sulak^e, S. Berkman^d, H.A. Tanaka^d,